

# Water Resources Research®

## RESEARCH ARTICLE





10.1029/2024WR037341

# Impact of Forest Dieback on Hydrology and Nitrogen Export Using a New Dynamic Water Quality Model



### Key Points:

- A dynamic water quality model is proposed to reproduce forest change processes in the simulation
- The modified model can capture the change of catchment runoff and nitrogen export before and after dieback and regeneration
- Forest dieback increases runoff by reducing evapotranspiration and increases nitrogen export by reducing uptake and increasing residues

Mufeng Chen<sup>1</sup> , Seifeddine Jomaa<sup>1</sup> , Angela Lausch<sup>2,3,4</sup> , Burkhard Beudert<sup>5</sup>, Salman Ghaffar<sup>1</sup>, Wenhao Jia<sup>6</sup>, and Michael Rode<sup>1,7</sup> 

<sup>1</sup>Department of Aquatic Ecosystem Analysis and Management, Helmholtz Centre for Environmental Research – UFZ, Magdeburg, Germany, <sup>2</sup>Department of Computational Landscape Ecology, Helmholtz Centre for Environmental Research – UFZ, Leipzig, Germany, <sup>3</sup>Department of Geography and Geoecology, Martin Luther University Halle-Wittenberg - MLU, Halle, Germany, <sup>4</sup>Department of Architecture, Facility Management and Geoinformation, Institute for Geoinformation and Surveying, Dessau, Germany, <sup>5</sup>Department of Conservation and Research, Bavarian Forest National Park, Grafenau, Germany, <sup>6</sup>Pearl River Water Resources Research Institute, Guangzhou, China, <sup>7</sup>Institute of Environmental Science and Geography, University of Potsdam, Potsdam-Golm, Germany

### Supporting Information:

Supporting Information may be found in the online version of this article.

### Correspondence to:

M. Chen and M. Rode,  
mufeng.chen@ufz.de; michael.rode@ufz.de

### Citation:

Chen, M., Jomaa, S., Lausch, A., Beudert, B., Ghaffar, S., Jia, W., & Rode, M. (2024). Impact of forest dieback on hydrology and nitrogen export using a new dynamic water quality model. *Water Resources Research*, 60, e2024WR037341. <https://doi.org/10.1029/2024WR037341>

Received 2 MAR 2024

Accepted 9 NOV 2024

### Author Contributions:

**Conceptualization:** Mufeng Chen, Michael Rode

**Data curation:** Mufeng Chen, Burkhard Beudert

**Methodology:** Mufeng Chen

**Resources:** Burkhard Beudert

**Supervision:** Seifeddine Jomaa,

Angela Lausch, Michael Rode

**Validation:** Salman Ghaffar, Wenhao Jia

**Writing – original draft:** Mufeng Chen

**Writing – review & editing:**

Seifeddine Jomaa, Wenhao Jia

**Abstract** Forest status is crucial for catchment hydrology and water quality but is increasingly disturbed by human activities and climatic factors. Therefore, it is urgently necessary to develop water quality models that can adapt to these changes. This study used a new dynamic Hydrological Predictions for the Environment (HYPE) model to assess the effect of rapid and continuous forest changes on catchment hydrology and nitrogen export. The modified HYPE model was implemented for the 25 years period in the Große Ohe catchment in Germany, which has experienced severe forest dieback and recovery. Due to the stochastic nature of infestation events, data covering the entire process of forest change are rare. The modified HYPE model performed well at different scales for discharge and dissolved inorganic nitrogen (DIN) export. It was able to (a) capture the timing of peak flows and the seasonal DIN concentration dynamics and (b) reflect the initial increase and subsequent decrease trend in discharge and DIN export in accordance with forest dieback and regeneration. The increase in nitrogen export after forest dieback primarily resulted from reduced forest uptake and increased soil nitrogen availability from tree residues. The difference in runoff and nitrogen export increment with or without regeneration highlights the importance of forest regeneration in restoring catchment hydrology and water quality. Additionally, a decrease in DIN export after residue removal implies the impact of sound post-disturbance management strategies. The dynamic modeling under changing catchment forests can enhance the analysis of catchment water quality and effectively support forest management.

## 1. Introduction

Forests play an important role in maintaining the health of ecosystems and mitigating climate change. However, forest dieback has been a significant problem in Central Europe since the 1970s, owing to the cumulative effects of atmospheric acid deposition (Bałazy et al., 2019). The degradation of forests continues to progress because of climate change, natural disasters, and anthropogenic logging and is of considerable concern (Patacca et al., 2023; Schuldt et al., 2020). Simultaneously, several management measures and natural evolutionary processes have contributed to the gradual regeneration of these forests (Ciais et al., 2008; Palmero-Iniesta et al., 2021). The impact of forest changes on hydrological processes and export of various nutrients from catchments has been the focus of hydrologists. It is also critical to further understanding and predicting the response of a catchment to forest changes, which can help us develop scientific forest management and ecological protection strategies.

Forest dieback impairs the original stable state of hydrology and water quality in catchments with mature forest (Brouillard et al., 2016) and alters its function in regulating water and nutrient cycling processes (Longo et al., 2020; Rodman et al., 2021). Forests influence catchment evapotranspiration and affect the timing and amount of precipitation entering the catchment hydrological cycle through canopy interception (de Oliveira et al., 2018; Page et al., 2020). Forest dieback can increase annual runoff and soil water content due to reduced canopy interception and evapotranspiration from canopy loss (Kopacek et al., 2020; Vilhar et al., 2022; Wickenkamp et al., 2016). However, recent studies have suggested that annual runoff may change little or decrease after forest loss, as reduced canopy interception and evapotranspiration can be compensated by increased soil evaporation, understory transpiration, and snowpack sublimation (Bennett et al., 2018; Bladon et al., 2019; McDowell et al., 2023). Similarly, the subsequent forest regeneration impacts can differ. Streamflow can either

© 2024. The Author(s).

This is an open access article under the terms of the [Creative Commons Attribution License](https://creativecommons.org/licenses/by/4.0/), which permits use, distribution and reproduction in any medium, provided the original work is properly cited.

increase or decrease, depending on factors such as time since disturbance, regeneration density and rate, and post-disturbance soil properties (Goeking & Tarboton, 2020; Kopáček et al., 2023; Veldkamp et al., 2020). Nitrogen cycling has similar variability in response to forest dieback and regeneration. Forests influence nitrogen cycling through nutrient supply, transport, and transformation of material and energy (Attiwill & Adams, 1993). Studies have shown that the decay of increased residues after forest dieback enriches soil nutrient pools, enhancing soil nitrogen mineralization and nitrification (Huber, 2005; Kopáček et al., 2023). Combined with reduced tree uptake, this leads to increased nitrogen loss from the catchment (Oulehle et al., 2019). Furthermore, the timing of increased nitrogen loss, especially nitrate nitrogen, can be controlled by the organic carbon content of added residues (Kaňa et al., 2015). However, previous studies also reported that soil nitrogen content and stream nitrate concentrations may remain unchanged or even decrease after forest mortality due to increased nitrogen uptake by understory plants (Mikkelsen et al., 2013; Schwendenmann & Michalzik, 2019). For regenerating forests, nitrogen loss decreases because of increased uptake demand and decreased nitrification rates compared to forest dieback period (Figueiredo et al., 2019). Nonetheless, soil nitrogen dynamics have been reported to differ with various regenerated tree species or regeneration strategies (Figueiredo et al., 2019; Liu et al., 2021; Ueda et al., 2017), leading to variation in soil nitrogen balance and transformation processes. Therefore, predicting the effects of forest change on runoff and nutrient export before and after forest dieback is crucial, but the long-term data to identify the processes are rare (Canelles et al., 2021).

Forest disturbances are becoming increasingly severe in Europe (Seidl et al., 2014), leading the hydrologic and water quality changes observable but can vary significantly in magnitude and timing (Georgiev et al., 2021; Paul et al., 2022), requiring timely and rational forest management (Kuuluvainen et al., 2021). This needs comprehending forest disturbance impacts over time and predicting the efficiency of management strategies. Hydrological and water quality models are commonly used for overall simulation and understanding processes (Abbott & Refsgaard, 1996), and the effects of different land use/cover conditions and their changes can also be investigated (Speich et al., 2020). Consideration of forest in these models is usually based on its role such as regulating hydrological processes, ecosystems, and material cycles (Sun et al., 2023). The effects of forest change are usually evaluated through comparative analysis of different forest cover scenarios, and forest change is often assumed to be a constant land cover pattern or a slow and gradual successional process over a long period (Jomaa et al., 2016; Kong et al., 2022; Thomas et al., 2021; Zhang et al., 2020). However, there is a lack of models and studies considering rapid and continuous forest changes due to disturbance in a single simulation. As a result, explorations of successive hydrological and water quality impacts at different stages after forest disturbance are rare. Given the importance of understanding these impacts for timely and appropriate management (Hlásny et al., 2021), there is a need to represent rapid forest change processes in hydrological models.

There are differences in the impacts of different forest disturbances. Forest mortality caused by insect infestation is increasing due to accelerating climate change, as well as natural disasters and land use change (Canelles et al., 2021; Kopáček et al., 2023). Unlike forest fires and harvesting, insect-induced forest dieback does not immediately and completely alter surface vegetation and soil surface properties or cause soil disturbances like compaction (Mikkelsen et al., 2013). The timescale for insect-induced forest dieback is often longer, which allows branches and trunks to continue intercepting precipitation and nutrient-rich tree debris to remain in place for decomposition (Mikkelsen et al., 2013; Vilhar et al., 2022). Some studies have discussed the effects of insect-induced tree mortality on hydrology and nutrients, their responses are close to the generalized perceptions, and also show variations across forests with different confounding factors such as surviving vegetation and climate conditions (Kopáček et al., 2023; Mikkelsen et al., 2013; Oulehle et al., 2019). However, due to the stochastic nature of these events there is still a lack of field investigations during the dieback and the recovery. This limits the use of models for understanding the nutrient turnover processes during the whole cycle of dieback and recovery. Our study sites Große Ohe and Forellenbach in the Bavarian Forest National Park (BFP) in Germany provide long term data and highly represent the features of the national park such as topography and vegetation cover, and forest mortality and regeneration processes (Klößing et al., 2007). This long-time data allows for combining field data with model simulations, offering a unique opportunity to analyze the effects of forest change.

In this study, we combined comprehensive observational pre- and post-forest mortality data with water quality modeling to enhance research on the impacts of insect-induced forest dieback and subsequent forest recovery, while advancing the development and application of water quality models. We aim to investigate how water quantity, quality, and key biogeochemical processes are changed by forest cover change after bark beetle disturbance with the comprehensive measured data. The objectives of this paper are to (a) improve the

**Table 1**  
*Physical Geography and Hydrometeorological Characteristics of Große Ohe and Forellenbach*

	Große Ohe	Forellenbach
Area (km <sup>2</sup> )	19.1	0.7
Elevation (m a.s.l.)	982 (770–1,447)	894 (787–1,293)
Slope (°)	11.1	8.4
Tree species in 1990 (%)	Norway spruce (70), broadleaves	Norway spruce (69), broadleaves
Soil (%)	Lithosols, rankers (16) Cambisols, podzols (60) Histosols, gleysols (23)	Lithosols, rankers (12) Cambisols, podzols (58) Histosols, gleysols (30)
Air temperature (°C)	5.4 (–20.2–26.8)	6.9 (–15.5–25.3)
Precipitation (mm a <sup>–1</sup> )	1,750 (1,210–2,400)	1,700 (1,190–2,400)
Runoff (mm a <sup>–1</sup> )	967 (590–1,720)	910 (690–1,500)

*Note.* Mean air temperature, mean precipitation, and runoff cover, 1991–2015.

hydrological model Hydrological Predictions for the Environment (HYPE) to dynamically simulate rapid and significant forest change, thereby enriching tools for studying the impacts of forest change; (b) based on model simulation and observation data, analyze the impact of forest dieback and regeneration on hydrology and nitrogen export; and (c) response of important hydrological and nitrogen processes, catchment runoff and nitrogen export to the forest dieback, regeneration and forest management practices.

## 2. Material and Method

### 2.1. Study Area and Data

Große Ohe is a headwater catchment of the Ilz-Danube River, located in the center of the BFNP, Germany. Forellenbach, a nested catchment in Große Ohe, is located in the southeast and covers 0.7 km<sup>2</sup> (Table 1; Figures 1a and 1b). The Große Ohe and Forellenbach catchments represent 7.6% and 0.3% of the Bavarian Forest, respectively, and are highly representative of its altitude distribution and all typical of habitats and ecosystems (Klößing et al., 2007). The tree species composition in the Große Ohe catchment also corresponds to that of the national park. Approximately 98% of Große Ohe is covered with forest dominated by Norway spruce (*Picea abies* (L.) Karst.) and European beech (*Fagus sylvatica* L.). The bedrock is composed of crystalline rocks (i.e., biotite granite and cordierite gneiss). Predominant soils in the area are acid cambisols with varying contents of coarse material and with differently marked signs of podsolization, rankers, and initial soils developed on autochthonous regolith and allochthonous periglacial cover beds. The slopes are primarily covered by cambisols, and bogs and mineral wet soils are dominant along streams and valleys.

Since the establishment of the national park in the 1970s, this area has remained unmanaged to prioritize natural processes in accordance with the “leaving nature alone” directive of the World Nature Protection Organization. At the end of the 20th century, the forest became vulnerable due to aging and increased acid deposition. By the early 1990s, the combination of warm winters and summers and storm events allowed bark beetles to gain a foothold. The continued reproduction of the bark beetles has led to the death of the forest, which was initially slow but began accelerating in 1996 (Huber, 2005; Zimmermann et al., 2000). In the BFNP, the mean basal area of mature spruce forest was 46 m<sup>2</sup>/ha before the bark beetle outbreak in 1991, with 96.7% of the area covered by spruce, and overstory tree density was 262 stems/ha (median). After the outbreak in 2002, basal area was reduced to 2.5 m<sup>2</sup>/ha with 65% of the area covered by spruce, none of which was in the overstory (Zeppenfeld et al., 2015). Forest mortality in Große Ohe and Forellenbach reached annual maxima in 1999 and 2006, respectively, during two pest outbreaks: from 1992 to 2000 and from 2000 to 2015. By around 2010, there was approximately 58% forests dieback in the catchment (Beudert et al., 2015). After the disturbance, the previously old spruce forest with a beech understory has become a beech stand that is heavily regenerating with spruce.

The spatial distributions of land use and soil types in the study area were provided by the BFNP (Figures 1c and 1d). The climate data for Große Ohe, including daily precipitation, daily maximum, minimum and average temperatures, relative humidity, global radiation and wind speed, were also provided by the BFNP.

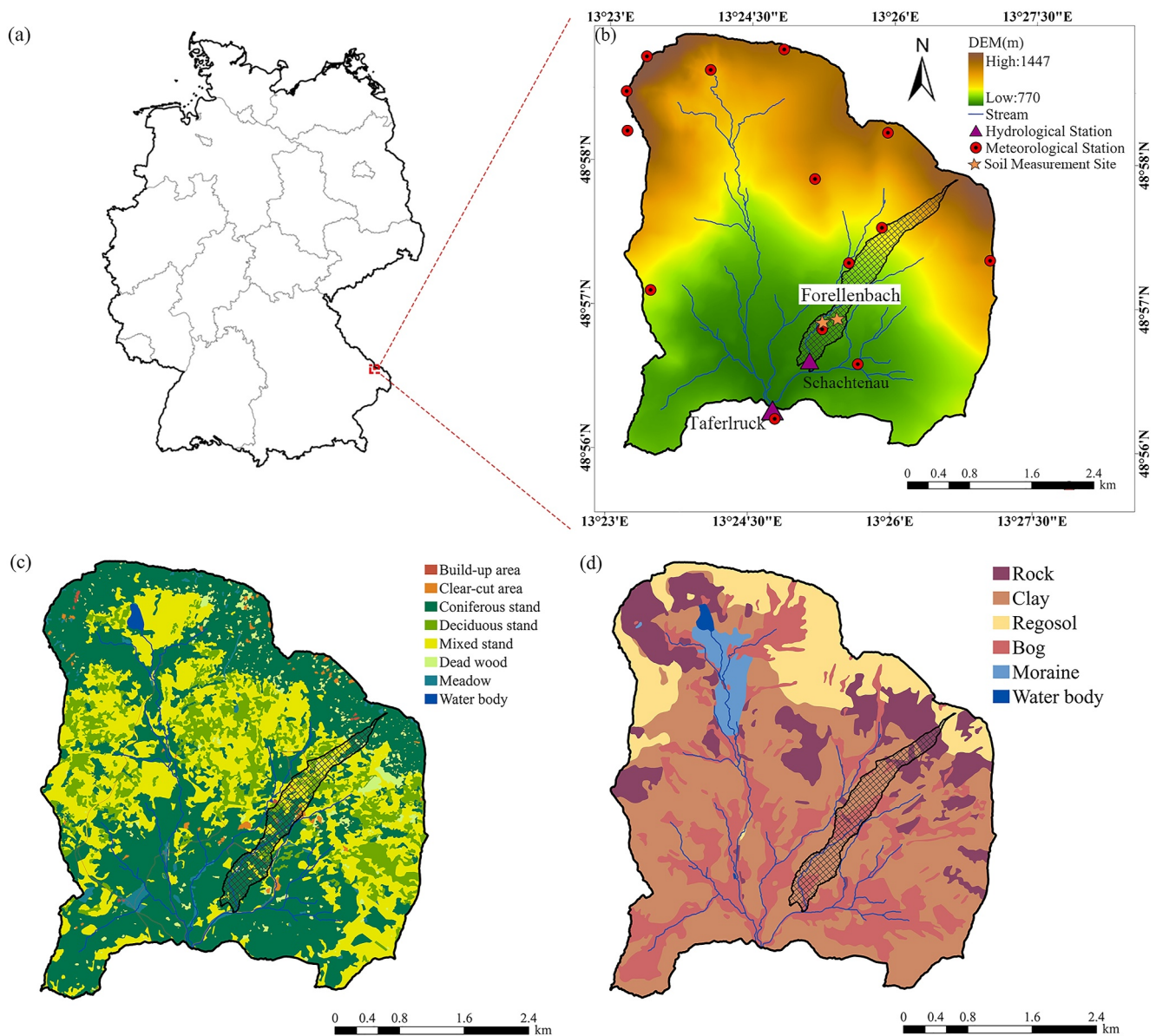


**Figure 1.** (a) Geographic location of Große Ohe and sub-catchment Forellenbach in the Bavarian National Park, Germany; (b) Digital Elevation Model and river network; (c) Land use types before 1990s; (d) Soil types.

The locations of the climate stations are shown in Figure 1b. The Bavarian Environmental Agency provides daily runoff and bi-weekly water chemistry data at the outlet of Große Ohe ( $48^{\circ}56'17.99''\text{N}$ ,  $13^{\circ}24'45.13''\text{E}$ , Taferlruck). Measurements in Forellenbach are a part of the UNECE ICP Integrated Monitoring program (<https://www.slu.se/en/Collaborative-Centres-and-Projects/integrated-monitoring>) under the 1979 Convention on Long-range Transboundary Air Pollution (<https://unece.org>). Daily runoff and weekly water chemistry data at its outlet ( $48^{\circ}56'33.61''\text{N}$ ,  $13^{\circ}25'10.63''\text{E}$ , Schachtenau) and data on weekly atmospheric deposition, monthly soil water and groundwater quantity, and water chemistry data were provided by the Federal Environmental Agency (UBA, 2022). The sum of ammonium nitrogen and nitrate nitrogen at the outlet was used to represent the inorganic nitrogen export from the catchment, hereafter collectively referred to as dissolved inorganic nitrogen (DIN). Forellenbach also has two soil monitoring sites located in the beech and spruce areas, that provide monthly soil water chemistry data for different soil layers. The soils of both observation sites are considered to be low nutrient, weakly podzolic acid brown soils developed on periglacial solifluction cover-bed. In 1996/1997, all spruce in the spruce intensive monitoring plot were killed by bark

**Table 2**  
*The Statistical Features of Observed Discharge, Dissolved Inorganic Nitrogen Concentrations and Nitrogen Export of Große Ohe and Forellenbach During the Study Period 1991–2015*

Catchment		Große Ohe	Forellenbach
Discharge (m <sup>3</sup> /s)	Range	0.09–11.9	$5.8 \times 10^{-3}$ –0.30
	Mean	0.59	0.02
	SD	0.66	0.02
DIN concentration (mg N/L)	Range	0.21–2.08	0.17–2.48
	Mean	1.00	1.14
	SD	0.27	0.46
Nitrogen export (kg N/ha/a)	Range	3.83–31.2	3.59–23.9
	Mean	11.9	10.6
	SD	7.15	4.99

*Note.* SD, Standard Deviation.

beetle infestation (Beudert & Breit, 2013b). The stock of coarse wood in the spruce area was about 998 VfmD/ha in 1995, but decreased by 99.8% to only 2 VfmD/ha after the bark beetle infestation. The number of living spruce trees decreased from 376/ha to 4/ha. The decrease in tree density significantly changed the forest canopy from closed to open, and subsequently again to a heterogeneously closed canopy due to numerous young regenerating spruces. The soil site with mature beech was not affected, with a stocker of 300 VfmD/ha in 1995, which was maintained at around 350 VfmD/ha in 2001. The living beech trees was 527/ha and 507/ha in 1995 and 2001, respectively (Beudert & Breit, 2013a). The UNECE ICP Integrated Monitoring program collected data on the annual nitrogen content of spruce and beech litter and the changes in spruce litter before and after the infestation and dieback due to bark beetles at these two measurement sites from 1992 to 2022.

The study period was from 1991 to 2015, considering the integrity of the data and the timing of bark beetle infestation events. The statistical features of daily discharge, DIN concentrations and nitrogen export of Große Ohe and Forellenbach during 1991–2015 are shown in Table 2 and Figure S1 in

Supporting Information S1. Discharge in both catchments was high in spring and winter and low in summer and autumn. The DIN concentrations in both catchments increased after 1997/1998 and peaked around 2003/2004. The concentration in Große Ohe was low during the growing season (May–September) and high during the rest of the year. In Forellenbach, the DIN concentration showed the same seasonal pattern as that of the entire Große Ohe before forest dieback intensified and DIN concentration increased; however, seasonality diminished thereafter, particularly in 2003 and 2004.

## 2.2. Dynamic Simulation HYPE Model

The semi-distributed model HYPE is an integrated process-oriented hydrological and water quality model developed by the Swedish Meteorological and Hydrological Institute (Lindstrom et al., 2010). The hydrological response unit for simulation in the HYPE model is the combination of different soil and land use types, referred to as soil and land cover classes (SLCs). The study catchment is first divided into sub-catchments, which are further divided into different SLCs. In each SLC, soil is divided into a maximum of three layers with different depth. Water flow and nitrogen concentrations are initially calculated for each soil layer and accumulated to the SLC scale, and then aggregated to the sub-catchment scale using area-weighted sums from the SLCs. Finally, each simulated variable is transferred between sub-catchments based on their connectivity and reaching the catchment's outlet. The information for each SLC in each sub-catchment is unique and is updated as the simulation progresses. HYPE operates with a daily time step, and the model equations are explicitly solved using the same time step.

Figure 2 illustrates the hydrological and nitrogen processes simulated within one SLC by HYPE. The hydrological processes include snowmelt, vegetation interception evaporation, evapotranspiration, surface runoff, infiltration, macropore flow, percolation, interflow, and groundwater flow. Vegetation transpiration and soil evaporation are jointly calculated as the function of air and soil temperature, and soil properties and moisture. Inorganic nitrogen (IN) and organic nitrogen (ON) are simulated as different soil immobile pools and dissolved substances in HYPE. Nitrogen transformation processes, including degradation, mineralization and denitrification, are simulated as functions of their transformation rate, available IN/ON pool, soil moisture and temperature, and, for denitrification, soil IN concentration. Plant uptake, calculated using logic uptake functions, is assumed to occur in the upper two soil layers and constrained by nitrogen availability. The basic equations used in HYPE can refer to Lindstrom et al. (2010).

In original HYPE, the characteristics of the SLCs are set before the simulation begins and remain unchanged to ensure consistency throughout the simulation. Our improved approach modifies the model setup strategy to ensure that it not only sets the catchment characteristics before the simulation begins but also checks for changes during the simulation and makes timely adjustments (Figure S2 in Supporting Information S1). In this study, the model checks for forest dieback or regeneration events before the simulation starts each year. If such events are

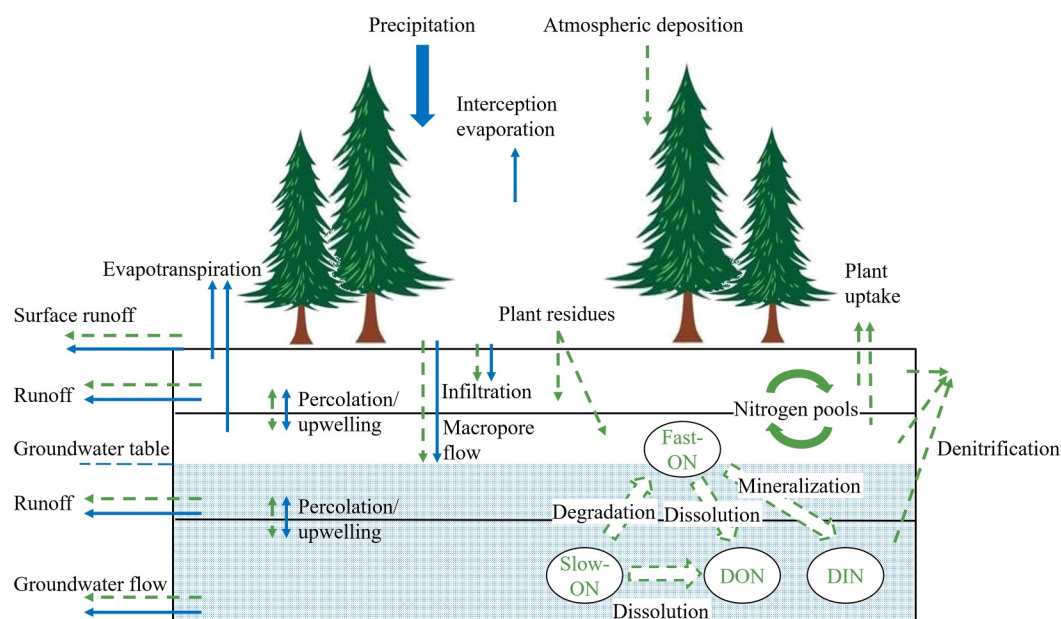


**Figure 2.** The hydrological and nitrogen processes simulated by the HYPE model. Green dashed lines represent nitrogen processes, while blue solid lines represent hydrological processes.

detected, the model updates the catchment forest cover status and continues simulations with the new catchment characteristics, including the types and area proportions of SLCs consisting of new forest status. Forest changes are evenly distributed within and between sub-catchments in the model, and are reflected by adjustments in area proportions of the SLCs consisting of different forest status. Previous studies indicate that without abrupt disturbances, variables such as soil moisture and nitrogen content should change gradually and remain constant within a day (Scheffer et al., 2001). For modeling, this implies that when using a daily calculation time step, the state variable values before forest change should be used as initial values for subsequent calculations in the areas undergoing forest change. To ensure this consistency before and after forest changes in the model, we propose a new attribute named “pre-state” for the new SLCs comprising new land use types. The “pre-state” indicates from which old SLC the new SLC was transformed, and the state variable value of the new SLC can be set based on its “pre-state.” In the model, information that needs to remain constant before and after forest changes primarily relates to the soil type in the SLC. This information is transferred to the new SLC based on the “pre-state” attribute. Parameters and settings related to land use type are determined based on the new land use type in the new SLC. After updating the distribution of new SLCs within each sub-catchment, the catchment characteristics are reset, and the land use change at the current time step is completed. The model then performs subsequent simulations based on the new catchment settings.

According to the HYPE model setup principles, the soil and land use types in Große Ohe were initially divided into 6 and 8 categories, respectively, and combined into 48 SLCs as calculation units. Considering the changing forest status, one land use type represented live spruces, and two more land use types were added later when the forest dieback and regeneration occurred, representing dead and regenerated spruces, respectively. According to Zeppenfeld et al. (2015), we assumed that all regenerated trees were spruce. Land use-dependent parameters may differ among these three types of forest status, reflecting the impact of forest changes. The interception loss (IL) rates were determined based on observed data. In the model, the nitrogen uptake of dead spruce was set to zero; nitrogen uptake in regenerated spruce occurs during the growing season (May to September). The amount of nitrogen uptake in regenerated spruce was estimated from the relationship among spruce biomass, nitrogen content, and tree age (Jacobsen et al., 2003; Wirth et al., 2004). The annual amount of litter produced by dead spruce was determined based on the observed data, and its decay process was calculated using a first-order exponential decay function (Olson, 1963; Zhang et al., 2008). The corresponding equations are listed in the

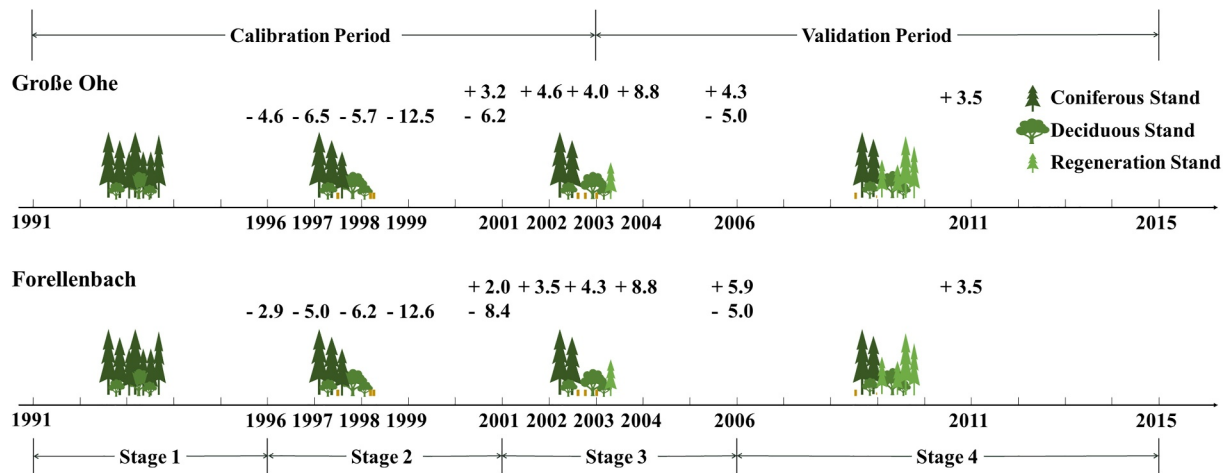


**Figure 3.** Assumptions for forest cover change in Große Ohe and Forellenbach for the model input and division of time periods. “-” and “+” indicate forest cover decrease and increase respectively; values refer to the proportion of forest cover change (%).

Supporting Information S1, the model can set the nitrogen supply for the soil in the years after spruce dieback based on the results. The litter produced by regenerated spruce was set to zero.

### 2.3. Forest Change Assumption and Scenario Analysis

To analyze the effects of forest cover change, we had to describe the natural succession process in the model. As mentioned in 2.2, forest coverage change was represented in the model as a percentage change in SLC, which is composed of various forest states, namely, live, dead, and regenerated spruces. Considering the complexity of the model setup, forest cover changes were set at several important time points. For forest dieback, the time and percentage decrease were set based on observed data and previous studies (Jung et al., 2021; Klöcking et al., 2005). For forest regeneration, we assumed that regeneration occurred in 70% of the dieback area 5 years after the dieback to the end of the study period (Heurich, 2009; Zeppenfeld et al., 2015). The assumed forest change processes in Große Ohe and Forellenbach are shown in Figure 3. Forest dieback and regeneration occurred in 1996–2006 and 2001–2011, with percentages ranging between 4.6%–12.5% and 3.2%–8.8% per year for Große Ohe and between 2.9%–12.6% and 2.0%–8.8% per year for Forellenbach, respectively (Figure 3).

To further elucidate the effects of forest cover change, we established three simulation scenarios (Scenario A–C) for comparison: forest unchanged (A), forest dieback only (B), and forest dieback and regeneration (C). The timing of forest dieback and regeneration was determined based on the actual conditions, with two dieback events beginning in 1996 and 2006 and regeneration beginning in 2001 (Figure 4). In addition, a fourth scenario, Scenario D, was established to elucidate the impact of different post-disturbance management approaches for dead trees on water quality in the catchment. Scenario D assumes that all remaining dead material will be removed, which will reduce the ground cover impact caused by undecomposed stems and branches and decrease additional nitrogen input. The year and percentage of forest dieback and regeneration in Scenario D were the same as in Scenario C (Figure 4). The study period was divided into four stages according to the start of forest dieback and regeneration in Große Ohe. The first stage (1991–1995) was before the first forest dieback when the state of the forest was the same for all scenarios; the second stage (1996–2000) was from the start of the first dieback until the start of regeneration, during which Scenarios B, C, and D experienced the same forest dieback during this period; the third stage (2001–2005) was from the start of forest regeneration until the start of the second forest dieback, during which Scenarios C and D experienced forest regeneration and Scenario B retained the dieback status; the fourth stage (2006–2015) began with the second forest dieback until the end of the entire period, during which Scenario B only experienced forest dieback, and Scenarios C and D experienced forest dieback and regeneration. Scenario A remained unaffected throughout the period and was used as a benchmark. All scenario simulations and comparisons were conducted at the scale of Große Ohe. We compared the discharge, DIN concentration, and nitrogen export under different forest change conditions (scenarios A, B, and C), DIN concentration and nitrogen export under different post-disturbance managements (scenarios C and D), and the overall change rate of hydrological and nitrogen key processes under different scenarios.

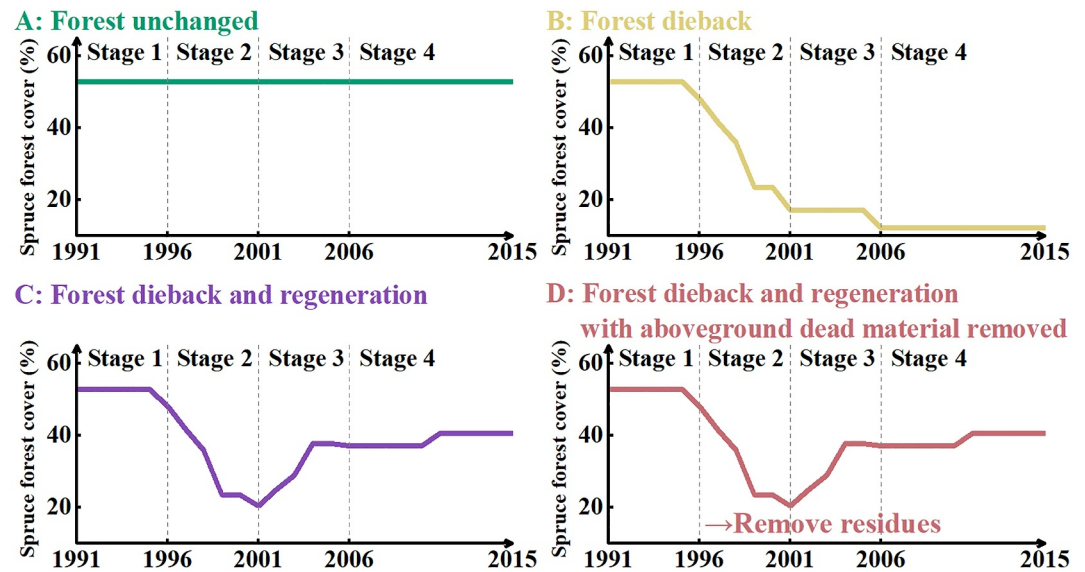


**Figure 4.** Forest cover change process in the four scenarios. Green: Scenario A (forest unchanged); yellow: Scenario B (forest dieback); purple: Scenario C (forest dieback and regeneration); brown: Scenario D (forest dieback and regeneration with aboveground dead material removed); Vertical dashed lines separate the four forest change stages.

## 2.4. Model Implementation

The main challenge in implementing the model is identifying its parameters. Therefore, we first conducted a sensitivity analysis to determine the most impactful parameters for calibration. These parameters were then calibrated based on three evaluation criteria. Finally, the model uncertainty was analyzed to assess the model's reliability.

### 2.4.1. Sensitivity Analysis

Parameters in the model represent the state of the modeled catchment or the coefficients of hydrological and nutrient transport and transformation processes. The outcome of these processes can vary by the soil and land use conditions. Due to the numerous processes involved in modeling catchment hydrology and nitrogen export and the variety of soil and land use types in the study area, the total number of parameters in our study was too extensive to calibrate. Therefore, a parameter sensitivity analysis was necessary to identify the parameters that have the most impact on the model output, and these parameters will be calibrated. To achieve this objective, the Sensitivity Analysis For Everybody (SAFE) toolbox developed by Pianosi et al. (2015) was adopted, and the global Elementary Effects Test (EET) evaluation method were applied by SAFE. The Latin hypercube sampling method and radial design were used to determine the initial random sample points in the decision space and change the locations of the samples. In the EET method, the elementary effects (EEs) of the  $j$ th parameter shifted from the  $i$ th sample point  $X_i$  are defined by Equation 1.

$$EE_{i,j}^k = \frac{f_k(x_{i,1}, x_{i,2} \dots x_{i,j-1}, x_{i,j} + \Delta, x_{i,j+1} \dots x_{i,d-1}, x_{i,d}) - f_k(X_i)}{\Delta} \quad (1)$$

where  $d$  is the dimension of sample  $X_i$ ;  $\Delta$  is the changing distance of parameter  $j$ ;  $f_k$  is the objective function showing the effect of parameter change, and  $k = 1, 2$  represents the Nash-Sutcliffe efficiency (NSE) and Kling-Gupta efficiency (KGE) (Gupta et al., 2009). The mean ( $\mu_j^k$ ) and standard deviation ( $\sigma_j^k$ ) of the EE for each parameter were first calculated based on the normalized  $EE_{i,j}^k$  of all sample points and then integrated to  $EE_{j,\mu}$  and  $EE_{j,\sigma}$  as indicators for sensitivity comparisons.



$$EE_{j,\mu} = \frac{1}{2} \sum_{k=1}^2 \mu_j^k = \frac{1}{2} \sum_{k=1}^2 \frac{1}{s} \sum_{i=1}^s |\text{norm}(EE_{i,j}^k)| \quad (2)$$

$$EE_{j,\sigma} = \frac{1}{2} \sum_{k=1}^2 \sigma_j^k = \frac{1}{2} \sum_{k=1}^2 \sqrt{\frac{1}{s-1} \sum_{i=1}^s (\text{norm}(EE_{i,j}^k) - \mu_j^k)^2} \quad (3)$$

where  $s$  is the number of sample points. When assessing the sensitivity of parameters, the higher the  $EE_{j,\mu}$  and  $EE_{j,\sigma}$ , the higher the sensitivity.

#### 2.4.2. Parameter Calibration With Multi-Objective Optimization

The most sensitive parameters were calibrated based on the sensitivity analysis results. The NSE is a commonly used criterion for model evaluation but may underestimate variability and water balance simulation (Pechlivanidis et al., 2011). The Percent Bias (PBIAS) criterion is used to reflect the cumulative deviation and simulated mass balance, and KGE can balance the evaluation of correlation, bias, and variability. Therefore, for a more comprehensive assessment, we used a multi-objective optimization method to calibrate the model. Three evaluation criteria—NSE, PBIAS, and KGE—were used as the objective functions, defined using Equations 4–6.

$$f_1 = \max \text{NSE} = \max \left\{ 1 - \frac{\sum_t^T (\text{Sim}(t) - \text{Obs}(t))^2}{\sum_t^T (\text{Obs}(t) - \overline{\text{Obs}})^2} \right\} \quad (4)$$

$$f_2 = \min \text{PBIAS} = \min \left| \frac{\sum_t^T (\text{Sim}(t) - \text{Obs}(t))}{\sum_t^T (\text{Obs}(t))} \right| \quad (5)$$

$$f_3 = \max \text{KGE} = \max \left\{ 1 - \sqrt{[1 - \text{corr}(\text{Sim}, \text{Obs})]^2 + \left[1 - \frac{\overline{\text{Sim}}}{\overline{\text{Obs}}}\right]^2 + \left[1 - \frac{\text{std}(\text{Sim})}{\text{std}(\text{Obs})}\right]^2} \right\} \quad (6)$$

where  $\text{Sim}(t)$ ,  $\text{Obs}(t)$  represents the simulated and observed values (discharge or nutrient concentration) at time step  $t$ ;  $\overline{\text{Sim}}$ ,  $\overline{\text{Obs}}$  represents the mean of the simulated and observed values;  $\text{corr}(\text{Sim}, \text{Obs})$  represents the correlation coefficient between the simulated and observed values; and  $\text{std}(\text{Sim})$  and  $\text{std}(\text{Obs})$  represent the standard deviations of the simulated and observed values, respectively.

The parameters associated with the hydrological and DIN processes were calibrated simultaneously for Große Ohe, Forellenbach, and the two soil measurement sites from 1991 to 2002. The calibration period encompasses the period before forest dieback and the processes of forest dieback and regeneration. This comprehensive timeframe allows for the calibration of parameters relevant to all forest status, both pre- and post-disturbance. The data series used for discharge calibration were daily discharge in Große Ohe and Forellenbach. For DIN concentration calibration, we compared the simulated data on the dates with observations with the corresponding observed data. The calibration data were bi-weekly DIN concentration in Große Ohe, weekly DIN concentration in Forellenbach and monthly DIN concentrations in different soil layers at the two soil measurement sites. To solve the multi-objective optimization calibration problem, we used the NSGA-III algorithm (Deb & Jain, 2014) and obtained the Pareto frontier, in which the number of iterations was set to 100 with 100 populations, and the total runs were 10,000. The optimal solution from the Pareto frontier was then selected based on the Euclidean distance from the ideal point. The point with the shortest distance from the ideal point was selected as the optimal solution, which corresponded to the parameter set with the best simulation results. The ideal points for each criterion were  $\text{NSE} = 1$ ,  $\text{PBIAS} = 0$ , and  $\text{KGE} = 1$ .

#### 2.4.3. Uncertainty Analysis

Model uncertainty results from the parameters, model structure, and data used for input and calibration (Moges et al., 2020; Wellen et al., 2015). In our model, the total and parameter uncertainties of the discharge and DIN concentration simulations were diagnosed using Differential Evolution Adaptive Metropolis (DREAM) (Vrugt

et al., 2009). The Markov Chain Monte Carlo approach was also integrated into this method for random sampling. To quantify the parameter uncertainty and total uncertainty of the model, we introduced evaluation criteria. The resolution of the confidence interval (CI) was assessed using average relative interval length (ARIL), and reliability was evaluated based on the proportion of observations included in the confidence interval (PCI) (Jin et al., 2010). We used the 95% CI for evaluation. The formulas for these indicators were defined using Equations 7 and 8.

$$\text{ARIL}_{95} = \frac{1}{n} \sum \frac{\text{Upper}(t)_{95} - \text{Lower}(t)_{95}}{\text{Obs}(t)} \quad (7)$$

$$\text{PCI}_{95} = \frac{\text{Nobs}_{95}}{n} \quad (8)$$

where the subscript 95 indicates that each criterion corresponds to the 95% CI;  $n$  is the number of observations;  $\text{Upper}(t)_{95}$  and  $\text{Lower}(t)_{95}$  are the upper and lower boundaries of the 95% CI, respectively; and  $\text{Nobs}_{95}$  is the number of observations within the 95% CI. Based on the given expression, the smaller the ARIL and the larger the PCI, the smaller the uncertainty of the model.

### 3. Results

#### 3.1. Model Parameter Analysis

The parameter sensitivity for the hydrology and nitrogen simulations was performed simultaneously, and the results are shown in Figure S3 in Supporting Information S1. The parameter controlling groundwater discharge ( $\text{rcgrw}$ ) had the highest sensitivity on discharge, followed by those related to evapotranspiration processes ( $\text{tmp}$  and  $\text{cevp}$ ), snow melt ( $\text{cmlt}$ ), soil effective porosity ( $\text{wcep}$ ), and soil wilting point ( $\text{wcwp}$ ). Because hydrological processes also affect the DIN concentration in streams, these aforementioned parameters are sensitive to both hydrological and nitrogen simulation. For the nitrogen simulation, the parameters with the highest sensitivity control the denitrification rate in the main stream ( $\text{denitwrm}$ ); the dissolution from the fast turnover labile organic nitrogen (fast-ON) to dissolved organic nitrogen ( $\text{dissolfn}$ ), which can change the available DIN pool in soil water; and the rate of mineralization ( $\text{minerfn}$ ) in soil from fast-ON to DIN. Of all the parameters dependent on soil, those related to clay were the most sensitive; of all the parameters dependent on land use, those related to coniferous or dead forest areas were the most sensitive. These results are consistent with the catchment condition that conifers occupy most of the catchment area, and that changes in forest status are the main reason for changes in hydrological and nitrogen processes.

According to the sensitivity analysis, the eight and five most important hydrological and nitrogen simulation parameters were selected, respectively, for model calibration and uncertainty analysis, of which two were general parameters, and the others were related to soil or land use. The initial ranges of these parameters were determined based on their physical meanings, literature review, settings in earlier versions of the model, and previous HYPE applications (Ghaffar et al., 2021; Jiang et al., 2014; Kong et al., 2022; Lindstrom et al., 2010). The description of these parameters and their optimal calibration values are presented in Table 3.

#### 3.2. Model Performance for Simulation of Discharge and DIN Concentration

The model performances for the simulations of discharge, DIN concentration, and export are presented in Table 4 and Figure 5 and Figure S4 in Supporting Information S1. For discharge, the simulation results (Figures 5a and 5b) and the values for the evaluation criteria showed that the model performed well on the Forellenbach and Große Ohe during the calibration (1991–2002) and validation (2003–2015) periods. The simulation results reflect the actual discharge processes and catchment water balance, as evidenced by the high NSE and KGE values and low PBIAS values. However, the model has underestimated some of the peak flows. This could result from the simplified snowmelt calculation method that relies only on temperature and neglect other environmental factors that can increase snowmelt amounts. Additionally, short-term, high-intensity rainfall at sub-daily scale and the resulting flooding events cannot be predicted precisely by the model with a daily time step, leading to underestimations of peak flows (Jiang et al., 2014).

**Table 3**  
*Calibrated Model Parameters and Their Optimal Values*

Parameter	Description	Initial range	Optimal value
Discharge parameters			
<i>rcgrw</i>	Runoff coefficient for regional groundwater flow (d <sup>-1</sup> )	[1 × 10 <sup>-4</sup> , 0.1]	0.027
<i>wcep</i>	Effective porosity as a fraction (–)		
Clay		[1 × 10 <sup>-3</sup> , 0.5]	0.058
<i>wcwp</i>	Wilting point as a fraction (–)		
Clay		[0, 0.5]	0.055
<i>tmp</i>	Threshold temperature for snow melt, snow density and evapotranspiration (°C)		
Dead forest		[–5, 5]	0.89
<i>cmlt</i>	Snow melting parameter (mm d <sup>-1</sup> °C <sup>-1</sup> )		
Coniferous forest		[0, 10]	5.00
Dead forest		[0, 10]	3.00
<i>cevp</i>	Potential evapotranspiration rate (mm d <sup>-1</sup> °C <sup>-1</sup> )		
Coniferous forest		[0.01, 1]	0.25
Dead forest		[0.01, 1]	0.16
DIN parameters			
<i>denitwrm</i>	Parameter for denitrification in main watercourse (kg m <sup>-2</sup> d <sup>-1</sup> )	[1 × 10 <sup>-6</sup> , 0.1]	0.003
<i>minerfn</i>	Mineralization of fast-ON to inorganic N (d <sup>-1</sup> )		
Coniferous forest		[1 × 10 <sup>-4</sup> , 0.8]	0.04
Dead forest		[1 × 10 <sup>-4</sup> , 0.8]	0.55
<i>dissolfn</i>	Decay of fast-ON to dissolved organic N (d <sup>-1</sup> )		
Coniferous forest		[0.01, 1]	0.4
Dead forest		[0.01, 1]	0.225

For nitrogen simulation, the model performed well with low PBIAS, and the high KGE values showed that the simulated values correlated well with the observations and could reflect the variability of the observed time series. The comparison of the simulated and measured time series of DIN concentrations (Figures 5c and 5d) demonstrated that the model could capture the values and variance of DIN concentrations and reflect the seasonal pattern within the study period in Große Ohe. For Forellenbach, concentration values were captured during the calibration and validation periods, and the seasonal pattern was reflected in the calibration period. During the

**Table 4**  
*Statistical Criteria (Nash-Sutcliffe Efficiency—NSE, Percent Bias—PBIAS and Kling-Gupta Efficiency—KGE) of Model Calibration and Validation for Daily Discharge, Bi-Weekly Dissolved Inorganic Nitrogen (DIN) Concentration and Nitrogen Export Simulations for Große Ohe Catchment and Weekly DIN Concentration and Nitrogen Export Simulations for Forellenbach Catchment*

	Catchment	Calibration (1991–2002)			Validation (2003–2015)		
		NSE	PBIAS (%)	KGE	NSE	PBIAS (%)	KGE
Discharge	Große Ohe	0.79	–6.00	0.74	0.75	–0.94	0.71
	Forellenbach	0.64	–5.90	0.61	0.63	–7.94	0.54
DIN concentration	Große Ohe	0.43	2.25	0.73	0.64	4.84	0.81
	Forellenbach	0.58	6.58	0.67	0.50	6.15	0.50
Nitrogen export	Große Ohe	0.80	–3.00	0.85	0.74	0.43	0.69
	Forellenbach	0.73	–9.10	0.75	0.56	–8.29	0.58

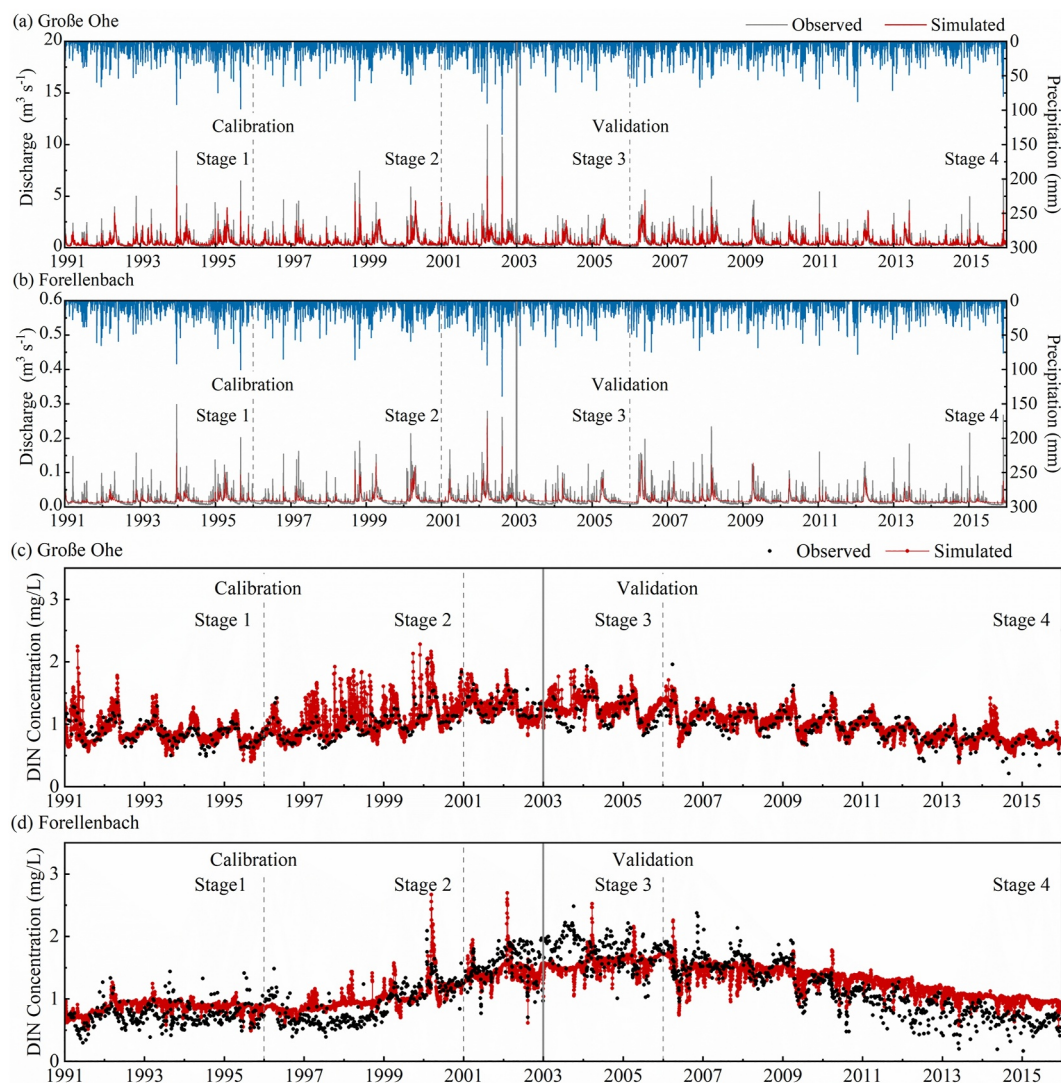


**Figure 5.** Model performances of discharge and dissolved inorganic nitrogen (DIN) concentration at the outlet of (a, c) Große Ohe and (b, d) Forellenbach during the calibration period (1991–2002) and validation period (2003–2015). Gray line: observed discharge, black dots: observed DIN concentration, red lines: simulated results, blue lines: precipitation, vertical dash lines separate the four forest change stages, and vertical solid lines separate calibration and validation periods.

validation period, the accuracy of the model in simulating seasonal characteristics was relatively low in the years when the seasonality of DIN concentrations changed, particularly in 2003 and 2004. Importantly, our modified HYPE model was able to simulate the overall trend of increasing and then decreasing DIN concentrations over the entire simulation period. For nitrogen export, the model accurately reflected the intra- and inter-annual variability in both catchments, as shown by the evaluation criteria and simulation process (Figure S4 in Supporting Information S1).

To determine whether the model could simulate nitrogen transformation and fluxes within the soil layers, we examined the monthly DIN concentrations in different soil layers at two measurement sites under spruce and beech. For Site 1 under spruce, which experienced tree death in 1996/1997, the simulation results reflected the observed rapid increase in the DIN concentration in each soil layer after the beginning of forest death. The values peaked approximately 2–3 years after the complete dieback of spruce but returned to their initial state after 5 years (Figure S5a in Supporting Information S1). The NSE was high in each soil layer, with values of 0.83, 0.67, and 0.83, respectively. For Site 2 under beech, we assumed that there was no forest cover change throughout the period, and the simulation reflected the changing range of the DIN concentration. Among the observations shown

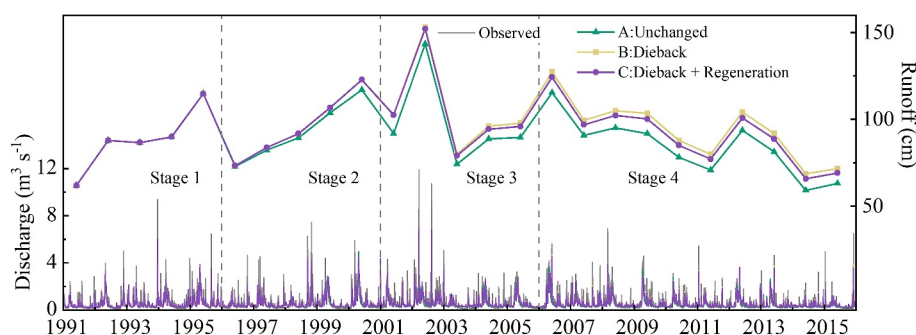


**Figure 6.** Daily discharge (left y-axis) and annual runoff (right y-axis) of the Große Ohe under scenarios A (forest unchanged, green), B (only forest dieback, yellow), and C (forest dieback and regeneration, purple).

in Figure S5b in Supporting Information S1, DIN concentrations around 2001 were higher than in other years, only these high values were not reflected in the simulation results.

### 3.3. Uncertainty Analysis

The parameter uncertainty of the discharge simulation was low, as reflected by the narrow CI band (black shaded area, Figure S6 in Supporting Information S1), which also shows variation similar to the observed data. The wider 95% CIs (gray shaded areas, Figure S6 in Supporting Information S1) and higher ARIL and PCI values (Table S1 in Supporting Information S1) for total uncertainty indicate greater uncertainty in the model structure and measurements than parametric uncertainty. Most of the observed discharge data at both catchment scales were covered by the total CI. In the DIN concentration simulation, the CI band was wider than in the discharge simulation, indicating a higher uncertainty. The parameter uncertainty was lower than the total uncertainty, suggesting that the uncertainties from the model structure and measurement errors were more significant. The total CI covered a large portion of the observed DIN concentration data in both catchments.

### 3.4. Hydrological Response to Forest Cover Change

The simulated daily discharge and annual runoff for the Scenarios A, B, and C are shown in Figure 6. The average annual runoff in Scenarios B and C was 7.00% and 5.41% higher than in Scenario A (885 mm), respectively. In general, catchment runoff increases due to the reduction in forest and then decreases when the forest begins to recover.

Figure 7 and Table S2 in Supporting Information S1 show the change rate of annual runoff, IL, ratio of IL to precipitation (IR), and actual total evapotranspiration minus canopy interception evaporation (ETA-IL) in Scenarios B and C, using Scenario A as the baseline. After forest dieback, IL, IR, and ETA-IL decreased and runoff increased. The difference between Scenarios B and C and Scenario A increased. As the forest began to regenerate, the original trends of these processes slowed down, and IL, IR, and ETA-IL began to increase, and runoff

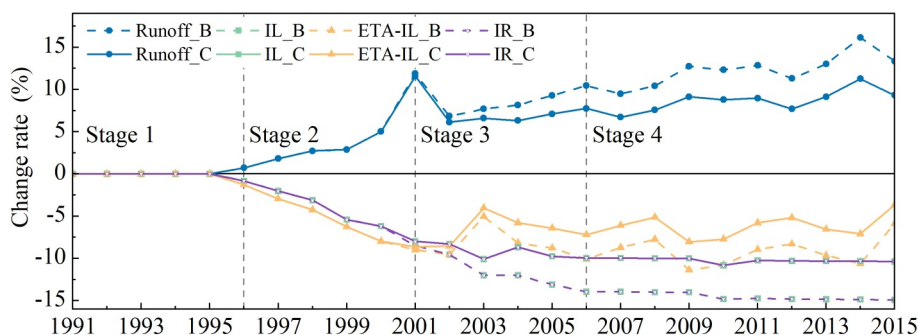


**Figure 7.** Change rate of runoff (blue), interception loss (IL, green), actual evapotranspiration without IL (ETA-IL, yellow), and ratio of IL to precipitation (IR, purple) in Scenarios B (forest dieback) and C (forest dieback and regeneration), using Scenario A (forest unchanged) as the baseline.

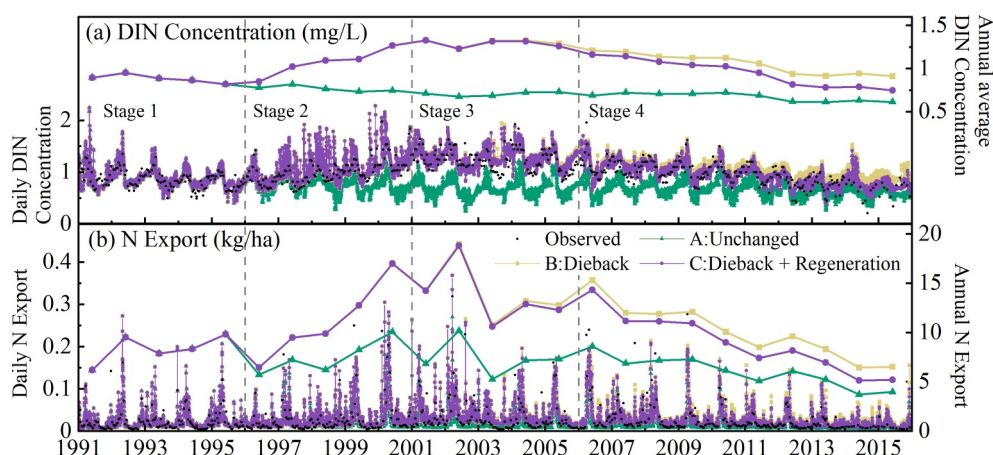


**Figure 8.** (a) Daily (left y-axis) and annual average (right y-axis) dissolved inorganic nitrogen (DIN) concentration and (b) Daily (left y-axis) and annual (right y-axis) nitrogen export of Große Ohe under Scenarios A (forest unchanged, green), B (only forest dieback, yellow) and, C (forest dieback and regeneration, purple).

decreased. The differences in these processes between Scenarios B and A were larger than those between Scenarios C and A.

The same change pattern was observed when comparing the runoff before and after tree mortality and regeneration within the complete forest change process in Scenario C. The hydrological process values were normalized to show their changes over the whole period (Figure S7 in Supporting Information S1), and the change rates of these processes in each stage compared with those of the previous stage were calculated (Table S3 in Supporting Information S1). The annual average runoff increased from Stage 1 to Stage 2, peaked at Stage 3, and then decreased at Stage 4 (Figure 6). Similar changes in IL and ETA-IL variability were also observed. After the expansion of dieback, IL, IR, and ETA-IL decreased. When regeneration began, ETA-IL increased and the decreasing trend of IR slowed down. At Stage 3, the slight increase in IL was mainly due to the high precipitation during this stage, but the difference was small.

Using Scenario A with forest unchanged, we can analyze the impact of climate conditions on hydrology. The change trends in annual precipitation and annual mean temperature were not significant during the study period. The correlation between temperature and annual runoff was weak, while the correlation between precipitation and annual runoff was strong, which aligns with general understanding. Relevant statistical results are shown in Table S4 in Supporting Information S1.

### 3.5. Nitrogen Export Response to Forest Cover Change

The DIN concentrations in catchment runoff and DIN export under the first three scenarios are shown in Figures 8a and 8b. The average annual DIN concentration in Scenarios B and C was 44.6% and 39.2% higher than in Scenario A (0.74 mg/L), respectively; and the annual nitrogen export in Scenarios B and C was 52.3% and 45.1% higher than in Scenario A (6.99 kg/ha/a), respectively.

Figure 9 and Table S2 in Supporting Information S1 show the change rate of annual soil denitrification (DENI), forest nitrogen uptake (FU), and mineralization that produce DIN (MINE) in Scenarios B and C, using Scenario A as the baseline. In general, owing to forest dieback, the loss of trees reduced the uptake of DIN from soil water, but the annual DENI and MINE in Scenarios B and C increased. The difference between Scenarios B and C and Scenario A increased with the expansion of forest dieback. When forest regeneration began, the consumption of DIN by FU increased, but the amount of nitrogen transformed in the soil decreased and gradually approached its initial state. After forest regeneration, the differences between Scenarios B and A were larger than those between Scenarios C and A.

The same change pattern of these processes was also observed before and after tree dieback and regeneration in Scenario C (Figure S8 and Table S3 in Supporting Information S1). The annual average DIN concentration and export increased after forest dieback at Stage 2 and reach to their peak at Stage 3, and then decreased at Stage 4

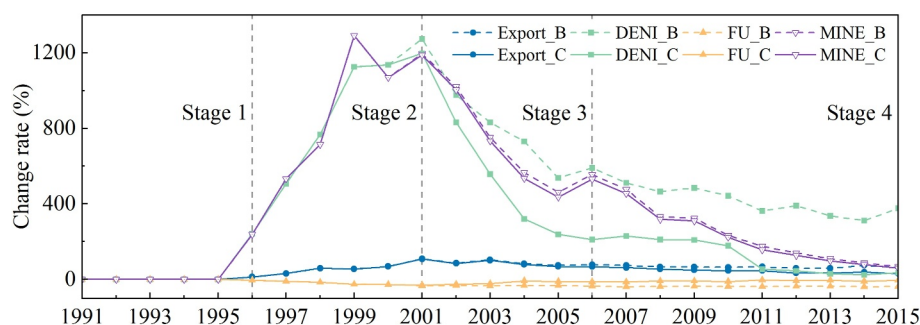


**Figure 9.** Change rate of export (blue), denitrification (DENI, green), forest nitrogen uptake (FU, yellow), and mineralization (MINE, purple) in Scenarios B (forest dieback) and C (forest dieback and regeneration) using Scenario A (forest unchanged) as the baseline.

(Figure 8). When forest dieback began, annual FU decreased, and annual DENI and MINE increased. After reforestation began, FU showed a stable increase, and DENI and MINE showed a continuous decrease.

The impact of climate conditions on DIN concentrations can be analyzed by Scenario A. The relationships between annual mean DIN concentration and both precipitation and temperature were weak, suggesting that DIN export was not significantly influenced by changes in climatic conditions during the study period.

### 3.6. Nitrogen Export Response to Post-Disturbance Management

The hydrological and nitrogen export processes under the two post-disturbance management methods are shown in Figure 10. In Scenario D, the average annual runoff is 3.64% higher than in Scenario C; the average annual DIN concentration and export are 27.4% and 25.5% lower than those in Scenario C. Using Scenario C as the baseline, the change rates between hydrological and nitrogen processes in Scenarios D and C are shown in Figure S9 and Table S5 in Supporting Information S1. Based on scenario assumptions and simulation results, reduced ground cover leads to lower interception losses and evapotranspiration, resulting in higher runoff. Additionally, the soil nitrogen pool shrank as the additional input from dead trees decreased, limiting all simulated nitrogen processes in the soil and reducing the nitrogen export from the catchment.

## 4. Discussion

### 4.1. Model Evaluation

The water and nitrogen cycles within a catchment are largely determined by its characteristics (Arheimer et al., 1996). With different or changing combination and distribution of forest cover in the catchment over time, we can observe the resulting changes of discharge and nitrogen export from the catchment. Due to the special bark beetle outbreaks in our study area, significant changes in hydrological conditions and nitrogen export from the catchment were observed within 25 years. These changes showed a rapid increase, followed by a gradual decrease to a level close to the original. The simulations confirm that our modified HYPE model reflects changes in water and nitrogen behaviors during different forest change stages. The calibration period comprises the time series from the beginning until the outbreak of bark beetles, and an early regeneration period. During this period, the model can simulate the regular processes before the outbreak, as well as the increase in discharge and surge in DIN concentration caused by forest dieback. The validation period includes the forest regeneration and the second bark beetle outbreak, during which the model can reflect the recovery of runoff and DIN concentration. Our improvements on the model dynamic setup strategy enabled it to adequately capture discharge and nitrogen processes, in turn demonstrating its ability to reflect rapid and long-lasting changes in land use.

The model performed better in simulating catchment runoff and nitrogen export at Große Ohe than at Forellenbach. The same was true for simulating the seasonal pattern of DIN concentrations, the model had difficulty reflecting the disordered seasonality in Forellenbach, especially during 2003/2004. This unclear seasonality of Forellenbach after forest disturbance was not an exception. This phenomenon has also been observed in other forested catchments, where large amounts of IN from dead tree residues alter the soil nitrogen balance and complicate the magnitude and temporal relationship between nitrogen mineralization and consumption year

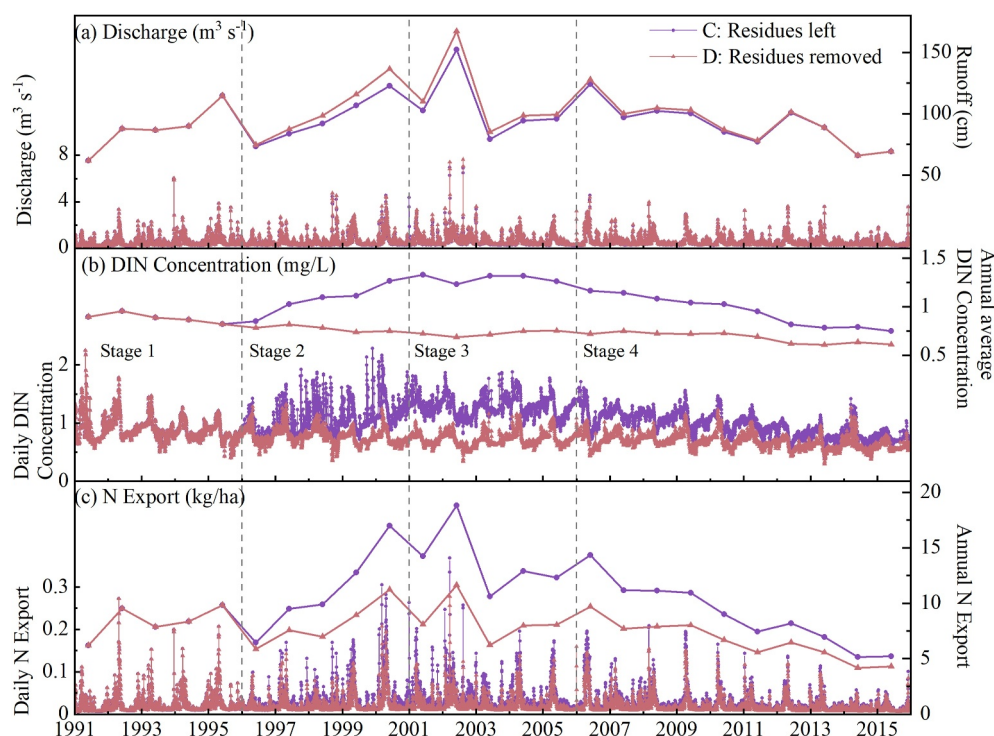


**Figure 10.** (a) Daily discharge (left y-axis) and annual runoff (right y-axis), (b) Daily (left y-axis) and annual average (right y-axis) dissolved inorganic nitrogen (DIN) concentration and (c) Daily (left y-axis) and annual (right y-axis) DIN export of Große Ohe under Scenarios C (with residues left, purple) and D (with residues removed, brown).

round (Ge et al., 2014; Pardo et al., 1995). Hence, drawing general conclusions is difficult due to the large variability between different catchments. To better capture their differences and enhance nitrogen transformation simulations, more site-specific data on deadwood residues and their decomposition processes would be beneficial. Additionally, improving soil process models by incorporating microbial biochemical interactions and accounting for interactions between nitrogen and other elements, such as carbon and phosphorus, could further refine simulation accuracy. However, the improved setting strategy and appropriate parameter set ensure that discharge, DIN concentration, and nitrogen export are well-represented throughout the study period.

The comparison between observations and simulations of soil water chemistry under spruce (Site 1) further demonstrates the ability of the model to capture internal processes, such as the transformation of nitrogen in the soil and its transfer between soil layers. Additionally, for Site 2 under beech, some outstanding values around 2001 could not be simulated well. Based on the BFNP observations and records, nitrogen leaching from the beech forest was minor. However, the spruce forest upstream of Site 2, also in Forellenbach, was killed by bark beetle infestation during 1999–2001, resulting in the leaching of DIN downstream through shallow groundwater flows (Beudert & Breit, 2013a). In the absence of specific data on how much nitrogen was leached downstream due to spruce mortality in the upstream area, we could not include this additional input in the model calculations. In addition, spatial explicit information within the sub-catchment is not considered in the semi-distributed model. The land use and soil characteristics are assumed to be homogeneously distributed across the sub-catchment, thus generalizing the connectivity and interactions between neighboring locations at the sub-catchment scale. Therefore, processes such as the lateral flow of soil water or groundwater within the sub-catchment cannot be represented by semi-distributed models.

In the uncertainty analysis, >95% of measured discharge and 93% of measured DIN concentration were covered by the 95% CIs. Compared with previous studies that used the original HYPE model (Ghaffar et al., 2021; Kong et al., 2022), our modified HYPE model is better in terms of uncertainty. Therefore, our improvements to the model structure are reasonable and can provide acceptable results for both hydrological and nitrogen simulations. However, further improvements to model performance could be achieved by using higher quality observation



data than used in this study, such as high-frequency data, because this type has been shown to reduce model uncertainty (Jiang et al., 2019; Piniewski et al., 2019).

#### 4.2. Impact of Forest Change on Hydrology

Comparisons among Scenarios A–C showed that changes in forest conditions affect the catchment runoff, and forest regeneration can mitigate the consequences of increased catchment runoff after forest dieback. Forest dieback reduces tree stands and canopy cover (Bernsteinová et al., 2015). On the one hand, forest transpiration was reduced or even ceased due to plant death and loss of canopy (Kopacek et al., 2020). On the other hand, the reduction in canopy cover reduces the amount of precipitation that returns directly to the atmosphere through interception evaporation, increasing the amount of precipitation that reaches the forest floor and contributes to flow-generating processes. Additionally, the simulation results for Scenario B and Stage 2 of Scenario C revealed that in temperate forests, forest dieback reduces IL to a greater extent than it reduces evapotranspiration. Previous studies have also supported this finding, showing that in dense forests with a high leaf area index ( $\text{m}^2$  leaf area per  $\text{m}^2$  ground), the rate and amount of interception evaporation are considerably greater than those of transpiration (Zheng & Jia, 2020). Therefore, changes in forest canopy cover are the most direct factor contributing to changes in catchment runoff (McDowell et al., 2023). In addition, the decrease in evaporation and transpiration losses from forest canopy is much larger than the increase in evapotranspiration of the soil and understory vegetation (Beudert et al., 2018; Klöcking et al., 2005). As a result, we can find the increase in surface runoff. By contrast, as forests regenerate and vegetation cover increase, interception evaporation and transpiration increase, leading to a reduction in runoff. The simulation results for Scenario B also indicate that IL has a greater response to forest regeneration compared to evapotranspiration. This finding is consistent with previous studies, which reported that forest regeneration also promotes hydrological recovery after forest dieback (Li et al., 2014; Wei & Zhang, 2010).

#### 4.3. Impact of Forest Change on Nitrogen Export

The differences between the simulation results under Scenarios A–C support the hypothesis that forest cover change affects catchment nitrogen export. Forest dieback increased nitrogen export from the catchment, and forest regeneration can reduce the export.

Generally, the biochemical processes related to soil DIN consumption and export include plant uptake and denitrification, and the main source of DIN is mineralization of ON (Persson et al., 2000). The Norway spruce forests can uptake nitrogen from soil in the form of  $\text{NH}_4^+$  or  $\text{NO}_3^-$  (Carlsson et al., 2017). Therefore, large-scale spruce forest mortality in the study area directly and immediately reduces the amount of DIN uptake. In the study area, after the death of spruce trees, their remains are unmanaged and decay naturally (Zimmermann et al., 2000). This process results in an increase in branches and needles as extra residues, which accelerates the decomposition of organic matter and microbial biomass, increasing the rate of nutrient turnover (Biederman et al., 2016; Peng et al., 2007). Thus, in Scenarios B and C with forest dieback, the annual mineralization and denitrification rates are higher than in the absence of forest disturbance. In addition, our simulations reveal that the soil mineralization process responded more quickly and strongly after forest dieback, but the period of excess mineralization also dissipated rapidly. Regarding the natural conditions of the study area, adequate precipitation ensures that biological activity is not water-limited and favors the rapid mineralization in soil (Dannenmann et al., 2016). However, this rapid mineralization response also leads to easily decomposable nitrogen-rich litter being quickly depleted by microbes, as evidenced by the sharp increase in mineralization and nitrogen export following forest dieback, and the rapid decline in mineralization after the end of the dieback period (year 2000 and 2006). Meanwhile, although denitrification was also shown to undergo significant changes, with a greater extent compared to uptake, the high permeability of the soil facilitates rapid loss of soil water and substances to the aquifer and streams, resulting in much less soil DIN being emitted to the atmosphere through denitrification than that retained, albeit also reduced, by forest uptake (Beudert et al., 2015). Soil DIN is moderated by the balance between removal and production (Fang et al., 2021), with reductions in DIN consumption and increases in production leading to the increase in soil leaching and the increase in nitrogen export from the catchment after forest dieback.

These processes above show opposing patterns of change as forests recover. Nitrogen is required for tree growth, which increases the consumption of DIN from soil water, reduces the soil DIN levels, and inhibits denitrification. Meanwhile, the amount of new litter falling to the ground in the regenerating forest is much lower, and the

remaining residues from the dead forest are gradually decomposed by biochemical processes and are nearly exhausted, thus decreasing the level of additional inputs. Consequently, the rates of soil nitrogen transformation processes decrease. Similar to the forest decline period, the decline in mineralized nitrogen coincided with a smaller denitrification rate compared to the increase in vegetation nitrogen uptake. This difference results in a final downward trend of DIN concentration and export. Furthermore, although the nitrogen export decreases without forest regeneration and the differences in nitrogen process rates between the scenarios with and without regeneration narrow due to the depletion of the residue supply, forest regeneration accelerates the recovery of nitrogen export from the catchment. It can be concluded that forest regeneration can improve the nitrogen retention capacity and water quality of the catchment by reducing nitrogen supply, increasing plant consumption, and decreasing the nitrogen conversion rate.

In addition, the climate impact on discharge or DIN concentrations was insignificant due to minimal climate change during the study period. However, recent changing climate has revealed dramatic impacts on forest cover and nutrient losses. For example, in temperate regions of central Germany, large-scale forest losses due to climate-induced bark beetle infestations can increase not only nitrogen and phosphorus losses to streams, but also eutrophication of reservoirs (Kong et al., 2022). More studies have shown that climate change affects forest cover and nutrient dynamics by altering physiological processes in trees, such as photosynthesis, and by enhancing environmental mortality drivers like natural disasters (Hartmann et al., 2022; Vacek et al., 2023). With the current warming climate, forest structure and carbon storage are predicted to be reorganized in the future (McDowell & Allen, 2015). Therefore, it is crucial to continue focusing on the impacts of climate change on forests.

#### 4.4. Impact of Forest Post-Disturbance Management

Salvage logging is a commonly used post-disturbance management method for restoring economic values and preventing post-disturbance risks (Müller et al., 2019). In our model simulation, the assumed post-disturbance management reduced stand trees and ground cover, thereby reducing interception and vegetation transpiration losses. As discussed above, increased surface exposure elevated ground evaporation, but vegetation transpiration had a greater impact on overall evapotranspiration, thus catchment runoff increased. For nitrogen export, nitrogen involved in the cycling processes of mineralization, denitrification, and tree uptake decreased, and the differences in their quantities resulted in a reduction in DIN concentration and export. Overall, the differences in catchment runoff and nitrogen export with or without post-disturbance management suggest that, in our case, post-disturbance interventions can help reduce excess nitrogen export from the catchment and mitigate pollution. In addition to the direct effect assumed in our scenario, hydrological and nitrogen processes can also be affected by heavy salvage logging machinery in actual post-disaster logging practices (Ibáñez et al., 2022; Zema, 2021). Heavy machinery can compact soil, reduce soil porosity, impair soil continuity, permeability (Nazari et al., 2021), and soil microbial activity and diversity. This leads to limited water infiltration, increased surface runoff (Shah et al., 2017), and inhibits plant uptake and nitrogen transformation (Longepierre et al., 2022; Shaheb et al., 2021; Tan et al., 2005). However, logging machinery has also been reported to promote nitrogen immobilization (Tian et al., 2012), and improve soil permeability by disrupting soil water repellency. From this perspective, logging techniques help to mitigate soil erosion and enhance soil and water conservation (Zema, 2021).

Thus, the effect of post-disturbance management, such as salvage logging, can be highly variable and site-specific. Experiments on forest soils burned in the Boggs Mountain Demonstration State Forest showed that post-disturbance logging compaction increased runoff by 41% and 127% in bare plots and mulched plots, respectively, compared to uncompacted counterparts (Prats et al., 2019). However, post-wildfire logging in western Montana significantly reduced runoff compared to no-harvest areas due to specific logging strategies, though soil erosion was similar in both areas (Robichaud et al., 2008). In contrast, experiments in the “Seich Sou” forest showed that logging after insect-induced forest death doubled the annual erosion rate compared to areas without logging (Kastridis et al., 2022). Similar variability can be observed for soil nitrogen. Soil nitrogen reduction after salvage logging was reported in the “Sierra de Mariola Natural Park” in Spain experienced forest fires (García-Orenes et al., 2017). However, an increase in resin-exchangeable nitrate and soil nitrogen leaching was observed downslope of the logged beetle-killed forest in the Arapaho-Roosevelt National Forest (Rhoades, 2019). By contrast, the experiment conducted in a Swedish boreal forest and the monitoring results of various streams in the BFNP revealed that the effects of salvage logging after wildfire and bark beetle infestation had no significant effect on nitrogen transformation or nitrate concentration (Georgiev et al., 2021;

Ibáñez et al., 2022), and maintained the water quality within the drinking water quality standards. Therefore, post-disturbance management decisions for affected forests should be made according to their specific environmental and disturbance characteristics, for which more data observations and scientific analyses are necessary.

## 5. Conclusions

The bark beetle-induced forest dieback in the Große Ohe catchment provided a valuable opportunity for analyzing catchment runoff and nitrogen export. Long-term time-series data allowed the integration of field observations with our modified HYPE model, which can dynamically describe forest change processes. By simulating catchment runoff, nitrogen export and their key processes, we analyzed the effects of forest dieback and regeneration on catchment hydrology and nitrogen export. The main conclusions include.

1. The modified HYPE model effectively simulated the impact of forest cover changes on DIN concentrations in different soil layers, as well as runoff and DIN export in both the Große Ohe and the Forellenbach catchments, demonstrating the validity of the model.
2. Canopy density affects evapotranspiration and IL and thus regulates runoff in the catchment after forest dieback and regeneration. Dead tree residues and plant nitrogen uptake are key factors influencing the nitrogen export of the catchment.
3. Post-disturbance management in our case can mitigate excess nitrogen export. However, as the effects of post-disturbance management vary greatly, effective implementation must be tailored to local conditions.

Our study points out the diversity of forest change impacts, showing the need for site-specific modeling to effectively capture these differences. At the same time, further research is required to investigate the combined effects of climate and forest change on catchment hydrology and nutrient losses, as well as management strategies for various forest conditions. Therefore, our modified HYPE model can serve as an effective tool for these investigations. In addition, the development of a comprehensive observational database is also an important future endeavor to support further research and improve our understanding of the effects of forest change.

## Conflict of Interest

The authors declare no conflicts of interest relevant to this study.

## Data Availability Statement

The streamflow and water quality data were provided from the Bavarian Environment Agency (LFU) and the German Federal Environment Agency (UBA) and are available online in Zenodo repository (<https://doi.org/10.5281/zenodo.14001652>; Chen, 2024b). The source code for the original HYPE model (version 5.18.0) is open access and available at <https://hypeweb.smhi.se/model-water/>, and the modified code is accessible at Chen (2024a).

## Acknowledgments

Mufeng Chen and Wenhao Jia are funded by the China Scholarship Council (CSC). Burkhard Beudert designed and implemented the water chemistry monitoring project in Forellenbach catchment and coordinated the related project in the Grosse Ohe catchment in the Bavarian Forest National Park. Michael Rode, Seifeddine Jomaa and Angela Lausch supervised this study and developed important concepts. Michael Rode and Mufeng Chen formulated research questions. Mufeng Chen developed the codes for improved model. Mufeng Chen performed the analysis and led the writing of the paper which all co-authors contributed to. Salman Ghaffar and Wenhao Jia supported the conception and model validation. Open Access funding enabled and organized by Projekt DEAL.

## References

- Abbott, M. B., & Refsgaard, J. C. (1996). *Distributed hydrological modelling*. Springer Science & Business Media.
- Arheimer, B., Andersson, L., & Lepisto, A. (1996). Variation of nitrogen concentration in forest streams influences of flow, seasonality and catchment characteristics. *Journal of Hydrology*, 179(1–4), 281–304. [https://doi.org/10.1016/0022-1694\(95\)02831-5](https://doi.org/10.1016/0022-1694(95)02831-5)
- Attwill, P. M., & Adams, M. A. (1993). Nutrient cycling in forests. *New Phytologist*, 124(4), 561–582. <https://doi.org/10.1111/j.1469-8137.1993.tb03847.x>
- Bałaży, R., Zasada, M., Ciesielski, M., Waraksa, P., & Zawila-Niedźwiecki, T. (2019). Forest dieback processes in the Central European Mountains in the context of terrain topography and selected stand attributes. *Forest Ecology and Management*, 435, 106–119. <https://doi.org/10.1016/j.foreco.2018.12.052>
- Bennett, K. E., Bohn, T. J., Solander, K., McDowell, N. G., Xu, C. G., Vivoni, E., & Middleton, R. S. (2018). Climate-driven disturbances in the San Juan River sub-basin of the Colorado River. *Hydrology and Earth System Sciences*, 22(1), 709–725. <https://doi.org/10.5194/hess-22-709-2018>
- Bernsteinová, J., Bässler, C., Zimmermann, L., Langhammer, J., & Beudert, B. (2015). Changes in runoff in two neighbouring catchments in the Bohemian Forest related to climate and land cover changes. *Journal of Hydrology and Hydromechanics*, 63(4), 342–352. <https://doi.org/10.1515/johh-2015-0037>
- Beudert, B., Bässler, C., Thorn, S., Noss, R., Schröder, B., Dieffenbach-Fries, H., et al. (2015). Bark beetles increase biodiversity while maintaining drinking water quality. *Conservation Letters*, 8(4), 272–281. <https://doi.org/10.1111/conl.12153>
- Beudert, B., Bernsteinová, J., Premier, J., & Bässler, C. (2018). Natural disturbance by bark beetle offsets climate change effects on streamflow in headwater catchments of the Bohemian Forest. *Silva Gabreta*, 24, 21–45.
- Beudert, B., & Breit, W. (2013a). Bodenchemische Veränderungen als Folge anthropogener Belastungen und natürlicher Störungen. *Hg. v. Nationalparkverwaltung Bayerischer Wald. im Auftrag des Umweltbundesamtes, Förderkennzeichen, 351(01)*, 012.

- Beudert, B., & Breit, W. (2013b). Soil chemical changes as a result of anthropogenic pollution and natural disturbances (Bodenchemische Veränderungen als Folge anthropogener Belastungen und natürlicher Störungen). *Hg. v. Nationalparkverwaltung Bayerischer Wald. im Auftrag des Umweltbundesamtes, Förderkennzeichen, 351(01)*, 012.
- Biederman, J. A., Meixner, T., Harpold, A. A., Reed, D. E., Gutmann, E. D., Gaun, J. A., & Brooks, P. D. (2016). Riparian zones attenuate nitrogen loss following bark beetle-induced lodgepole pine mortality. *Journal of Geophysical Research-Biogeosciences*, *121(3)*, 933–948. <https://doi.org/10.1002/2015jg003284>
- Bladon, K. D., Bywater-Reyes, S., LeBoldus, J. M., Kerö, S., Segura, C., Ritóková, G., & Shaw, D. C. (2019). Increased streamflow in catchments affected by a forest disease epidemic. *Science of the Total Environment*, *691*, 112–123. <https://doi.org/10.1016/j.scitotenv.2019.07.127>
- Brouillard, B. M., Dickenson, E. R. V., Mikkelsen, K. M., & Sharp, J. O. (2016). Water quality following extensive beetle-induced tree mortality: Interplay of aromatic carbon loading, disinfection byproducts, and hydrologic drivers. *Science of the Total Environment*, *572*, 649–659. <https://doi.org/10.1016/j.scitotenv.2016.06.106>
- Canelles, Q., Aquilué, N., James, P. M., Lawler, J., & Brotons, L. (2021). Global review on interactions between insect pests and other forest disturbances. *Landscape Ecology*, *36(4)*, 945–972. <https://doi.org/10.1007/s10980-021-01209-7>
- Carlsson, J., Svennerstam, H., Moritz, T., Egertsdotter, U., & Ganeteg, U. (2017). Nitrogen uptake and assimilation in proliferating embryonic cultures of Norway spruce—Investigating the specific role of glutamine. *PLoS One*, *12(8)*, e0181785. <https://doi.org/10.1371/journal.pone.0181785>
- Chen, M. (2024a). Improved HYPE model at time of publication. *Zenodo*. <https://doi.org/10.5281/zenodo.13363351>
- Chen, M. (2024b). The streamflow and water quality data for two catchments in the Bavarian Forest National Park, Germany [Dataset]. *Zenodo*. <https://doi.org/10.5281/zenodo.14001652>
- Ciais, P., Schelhaas, M.-J., Zaehle, S., Piao, S., Cescatti, A., Liski, J., et al. (2008). Carbon accumulation in European forests. *Nature Geoscience*, *1(7)*, 425–429. <https://doi.org/10.1038/ngeo233>
- Dannenmann, M., Bimüller, C., Gschwendtner, S., Leberecht, M., Tejedor, J., Bilela, S., et al. (2016). Climate change impairs nitrogen cycling in European Beech forests. *PLoS One*, *11(7)*, e0158823. <https://doi.org/10.1371/journal.pone.0158823>
- Deb, K., & Jain, H. (2014). An evolutionary many-objective optimization algorithm using reference-point-based nondominated sorting approach, Part I: Solving problems with box constraints. *IEEE Transactions on Evolutionary Computation*, *18(4)*, 577–601. <https://doi.org/10.1109/TEVC.2013.2281535>
- de Oliveira, J. V., Ferreira, D. B. d. S., Sahoo, P. K., Sodr e, G. R. C., de Souza, E. B., & Queiroz, J. C. B. (2018). Differences in precipitation and evapotranspiration between forested and deforested areas in the Amazon rainforest using remote sensing data. *Environmental Earth Sciences*, *77(6)*, 239. <https://doi.org/10.1007/s12665-018-7411-9>
- Fang, X.-M., Wang, G. G., Xu, Z.-J., Zong, Y.-Y., Zhang, X.-L., Li, J.-J., et al. (2021). Litter addition and understory removal influenced soil organic carbon quality and mineral nitrogen supply in a subtropical plantation forest. *Plant and Soil*, *460(1–2)*, 527–540. <https://doi.org/10.1007/s11104-020-04787-8>
- Figueiredo, V., Enrich-Prast, A., & Rütting, T. (2019). Evolution of nitrogen cycling in regrowing Amazonian rainforest. *Scientific Reports*, *9(1)*, 8538. <https://doi.org/10.1038/s41598-019-43963-4>
- García-Orenes, F., Arcenegui, V., Chrenková, K., Mataix-Solera, J., Moltó, J., Jara-Navarro, A. B., & Torres, M. (2017). Effects of salvage logging on soil properties and vegetation recovery in a fire-affected mediterranean forest: A two year monitoring research. *Science of the Total Environment*, *586*, 1057–1065. <https://doi.org/10.1016/j.scitotenv.2017.02.090>
- Ge, P., Da, L., Wang, W., & Xu, X. (2014). Seasonal dynamics of dissolved organic carbon, nitrogen and other nutrients in soil of Pinus massoniana stands after pine wilt disease disturbance. *Journal of Soil Science and Plant Nutrition*, *14(1)*, 75–87. <https://doi.org/10.4067/S0718-95162014005000006>
- Georgiev, K. B., Beudert, B., Bässler, C., Feldhaar, H., Heibl, C., Karasch, P., et al. (2021). Forest disturbance and salvage logging have neutral long-term effects on drinking water quality but alter biodiversity. *Forest Ecology and Management*, *495*, 119354. <https://doi.org/10.1016/j.foreco.2021.119354>
- Ghaffar, S., Jomaa, S., Meon, G., & Rode, M. (2021). Spatial validation of a semi-distributed hydrological nutrient transport model. *Journal of Hydrology*, *593*, 125818. <https://doi.org/10.1016/j.jhydrol.2020.125818>
- Goeking, S. A., & Tarboton, D. G. (2020). Forests and water yield: A synthesis of disturbance effects on streamflow and snowpack in western coniferous forests. *Journal of Forestry*, *118(2)*, 172–192. <https://doi.org/10.1093/jofore/fvz069>
- Gupta, H. V., Kling, H., Yilmaz, K. K., & Martinez, G. F. (2009). Decomposition of the mean squared error and NSE performance criteria: Implications for improving hydrological modelling. *Journal of Hydrology*, *377(1–2)*, 80–91. <https://doi.org/10.1016/j.jhydrol.2009.08.003>
- Hartmann, H., Bastos, A., Das, A. J., Esquivel-Muelbert, A., Hammond, W. M., Martínez-Vilalta, J., et al. (2022). Climate change risks to global forest health: Emergence of unexpected events of elevated tree mortality worldwide. *Annual Review of Plant Biology*, *73(1)*, 673–702. <https://doi.org/10.1146/annurev-arplant-102820-012804>
- Heurich, M. (2009). Progress of forest regeneration after a large-scale Ips typographus outbreak in the subalpine Picea abies forests of the Bavarian Forest National Park. *Silva Gabreta*, *15(1)*, 49–66.
- Hlásny, T., König, L., Krokene, P., Lindner, M., Montagné-Huck, C., Müller, J., et al. (2021). Bark beetle outbreaks in Europe: State of knowledge and ways forward for management. *Current Forestry Reports*, *7(3)*, 138–165. <https://doi.org/10.1007/s40725-021-00142-x>
- Huber, C. (2005). Long lasting nitrate leaching after bark beetle attack in the highlands of the Bavarian Forest National Park. *Journal of Environmental Quality*, *34(5)*, 1772–1779. <https://doi.org/10.2134/jeq2004.0210>
- Ibáñez, T. S., Rütting, T., Nilsson, M., Wardle, D. A., & Gundale, M. (2022). Mid-term effects of wildfire and salvage logging on gross and net soil nitrogen transformation rates in a Swedish boreal forest. *Forest Ecology and Management*, *517*, 120240. <https://doi.org/10.1016/j.foreco.2022.120240>
- Jacobsen, C., Rademacher, P., Meesenburg, H., & Meiwes, K. (2003). Gehalte chemischer Elemente in Baumkompartimenten. Literaturstudie und Datensammlung. *Berichte des Forschungszentrums Waldökosysteme, Reihe B*, *69*, 1–81.
- Jiang, S., Jomaa, S., & Rode, M. (2014). Modelling inorganic nitrogen leaching in nested mesoscale catchments in central Germany. *Ecology*, *7(5)*, 1345–1362. <https://doi.org/10.1002/eco.1462>
- Jiang, S., Zhang, Q., Werner, A., Wellen, C., Jomaa, S., Zhu, Q., et al. (2019). Effects of stream nitrate data frequency on watershed model performance and prediction uncertainty. *Journal of Hydrology*, *569*, 22–36. <https://doi.org/10.1016/j.jhydrol.2018.11.049>
- Jin, X. L., Xu, C. Y., Zhang, Q., & Singh, V. P. (2010). Parameter and modeling uncertainty simulated by GLUE and a formal Bayesian method for a conceptual hydrological model. *Journal of Hydrology*, *383(3–4)*, 147–155. <https://doi.org/10.1016/j.jhydrol.2009.12.028>

- Jomaa, S., Jiang, S. Y., Thraen, D., & Rode, M. (2016). Modelling the effect of different agricultural practices on stream nitrogen load in central Germany. *Energy Sustainability and Society*, 6(11), 11. <https://doi.org/10.1186/s13705-016-0077-9>
- Jung, H., Senf, C., Beudert, B., & Krueger, T. (2021). Bayesian hierarchical modeling of nitrate concentration in a forest stream affected by large-scale forest dieback. *Water Resources Research*, 57(2), e2020WR027264. <https://doi.org/10.1029/2020WR027264>
- Kaňa, J., Tahovská, K., Kopáček, J., & Šantrůčková, H. (2015). Excess of organic carbon in mountain spruce forest soils after bark beetle outbreak altered microbial N transformations and mitigated N-saturation. *PLoS One*, 10(7), e0134165. <https://doi.org/10.1371/journal.pone.0134165>
- Kastridis, A., Stathis, D., Sapountzis, M., & Theodosiou, G. (2022). Insect outbreak and long-term post-fire effects on soil erosion in mediterranean suburban forest. *Land*, 11(6), 911. <https://doi.org/10.3390/land11060911>
- Klöcking, B., Beudert, B., Lasch, P., Suckow, F., & Schwarze, R. (2007). Auswirkung von Störungen auf den Wasser- und Stoffhaushalt eines bewaldeten Einzugsgebietes: Monitoring und Modellierung. *diesem Band*.
- Klöcking, B., Schwarze, R., Beudert, B., Suckow, F., Lasch, P., Badeck, F., & Pfützner, B. (2005). Effects of bark beetle infestation on the water and matter balance of two water catchment areas in the Bavarian Forest National Park (Auswirkungen des Borkenkäferbefalls auf den Wasser- und Stoffhaushalt zweier Gewässereinzugsgebiete im Nationalpark Bayerischer Wald). *Nationalparkverwaltung Bayerischer Wald*.
- Kong, X. Z., Ghaffar, S., Determann, M., Friese, K., Jomaa, S., Mi, C. X., et al. (2022). Reservoir water quality deterioration due to deforestation emphasizes the indirect effects of global change. *Water Research*, 221, 118721. <https://doi.org/10.1016/j.watres.2022.118721>
- Kopáček, J., Bače, R., Choma, M., Hejzlar, J., Kaňa, J., Oulehle, F., et al. (2023). Carbon and nutrient pools and fluxes in unmanaged mountain Norway spruce forests, and losses after natural tree dieback. *Science of the Total Environment*, 903, 166233. <https://doi.org/10.1016/j.scitotenv.2023.166233>
- Kopacek, J., Bace, R., Hejzlar, J., Kana, J., Kucera, T., Matejka, K., et al. (2020). Changes in microclimate and hydrology in an unmanaged mountain forest catchment after insect-induced tree dieback. *Science of the Total Environment*, 720, 137518. <https://doi.org/10.1016/j.scitotenv.2020.137518>
- Kuuluvainen, T., Angelstam, P., Frelich, L., Jögiste, K., Koivula, M., Kubota, Y., et al. (2021). Natural disturbance-based forest management: Moving beyond retention and continuous-cover forestry. *Frontiers in Forests and Global Change*, 4, 629020. <https://doi.org/10.3389/ffgc.2021.629020>
- Li, S., Xu, M., & Sun, B. (2014). Long-term hydrological response to reforestation in a large watershed in southeastern China. *Hydrological Processes*, 28(22), 5573–5582. <https://doi.org/10.1002/hyp.10018>
- Lindstrom, G., Pers, C., Rosberg, J., Stromqvist, J., & Arheimer, B. (2010). Development and testing of the HYPE (Hydrological Predictions for the Environment) water quality model for different spatial scales. *Hydrology Research*, 41(3–4), 295–319. <https://doi.org/10.2166/nh.2010.007>
- Liu, S., Luo, D., Cheng, R., Wu, J., Yang, H., & Shi, Z. (2021). Temporal variability in soil net nitrogen mineralization among forest regeneration patterns in eastern Tibetan Plateau. *Ecological Indicators*, 128, 107811. <https://doi.org/10.1016/j.ecolind.2021.107811>
- Longepierre, M., Feola Conz, R., Barthel, M., Bru, D., Philippot, L., Six, J., & Hartmann, M. (2022). Mixed effects of soil compaction on the nitrogen cycle under pea and wheat. *Frontiers in Microbiology*, 12, 822487. <https://doi.org/10.3389/fmicb.2021.822487>
- Longo, M., Saatchi, S., Keller, M., Bowman, K., Ferraz, A., Moorcroft, P. R., et al. (2020). Impacts of degradation on water, energy, and carbon cycling of the Amazon tropical forests. *Journal of Geophysical Research: Biogeosciences*, 125(8), e2020JG005677. <https://doi.org/10.1029/2020jg005677>
- McDowell, N. G., & Allen, C. D. (2015). Darcy's law predicts widespread forest mortality under climate warming. *Nature Climate Change*, 5(7), 669–672. <https://doi.org/10.1038/nclimate2641>
- McDowell, N. G., Anderson-Teixeira, K., Biederman, J. A., Breshears, D. D., Fang, Y., Fernandez-de-Una, L., et al. (2023). Ecohydrological decoupling under changing disturbances and climate. *One Earth*, 6(3), 251–266. <https://doi.org/10.1016/j.oneear.2023.02.007>
- Mikkelsen, K. M., Bearup, L. A., Maxwell, R. M., Stednick, J. D., McCray, J. E., & Sharp, J. O. (2013). Bark beetle infestation impacts on nutrient cycling, water quality and interdependent hydrological effects. *Biogeochemistry*, 115(1–3), 1–21. <https://doi.org/10.1007/s10533-013-9875-8>
- Moges, E., Demissie, Y., Larsen, L., & Yassin, F. (2020). Sources of hydrological model uncertainties and advances in their analysis. *Water*, 13(1), 28. <https://doi.org/10.3390/w13010028>
- Müller, J., Noss, R. F., Thorn, S., Bäessler, C., Leverkus, A. B., & Lindenmayer, D. (2019). Increasing disturbance demands new policies to conserve intact forest. *Conservation Letters*, 12(1), e12449. <https://doi.org/10.1111/conl.12449>
- Nazari, M., Eteghadipour, M., Zarebanadkouki, M., Ghorbani, M., Dippold, M. A., Bilyera, N., & Zamanian, K. (2021). Impacts of logging-associated compaction on forest soils: A meta-analysis. *Frontiers in Forests and Global Change*, 4, 780074. <https://doi.org/10.3389/ffgc.2021.780074>
- Olson, J. S. (1963). Energy storage and the balance of producers and decomposers in ecological systems. *Ecology*, 44(2), 322–331. <https://doi.org/10.2307/1932179>
- Oulehle, F., Wright, R. F., Svoboda, M., Bace, R., Matejka, K., Kana, J., et al. (2019). Effects of bark beetle disturbance on soil nutrient retention and lake chemistry in glacial catchment. *Ecosystems*, 22(4), 725–741. <https://doi.org/10.1007/s10021-018-0298-1>
- Page, T., Chappell, N. A., Beven, K. J., Hankin, B., & Kretzschmar, A. (2020). Assessing the significance of wet-canopy evaporation from forests during extreme rainfall events for flood mitigation in mountainous regions of the United Kingdom. *Hydrological Processes*, 34(24), 4740–4754. <https://doi.org/10.1002/hyp.13895>
- Palmero-Iniesta, M., Pino, J., Pesquer, L., & Espelta, J. M. (2021). Recent forest area increase in Europe: Expanding and regenerating forests differ in their regional patterns, drivers and productivity trends. *European Journal of Forest Research*, 140(4), 793–805. <https://doi.org/10.1007/s10342-021-01366-z>
- Pardo, L., Driscoll, C., & Likens, G. (1995). Patterns of nitrate loss from a chronosequence of clear-cut watersheds. *Water, Air, and Soil Pollution*, 85(3), 1659–1664. <https://doi.org/10.1007/BF00477218>
- Patacca, M., Lindner, M., Lucas-Borja, M. E., Cordonnier, T., Fidej, G., Gardiner, B., et al. (2023). Significant increase in natural disturbance impacts on European forests since 1950. *Global Change Biology*, 29(5), 1359–1376. <https://doi.org/10.1111/gcb.16531>
- Paul, M., LeDuc, S., Lassiter, M., Moorhead, L., Noyes, P., & Leibowitz, S. (2022). Wildfire induces changes in receiving waters: A review with considerations for water quality management. *Water Resources Research*, 58(9), e2021WR030699. <https://doi.org/10.1029/2021wr030699>
- Pechlivanidis, I., Jackson, B., McIntyre, N., & Wheat, H. (2011). Catchment scale hydrological modelling: A review of model types, calibration approaches and uncertainty analysis methods in the context of recent developments in technology and applications. *Global NEST journal*, 13(3), 193–214. <https://doi.org/10.30955/gnj.000778>
- Peng, Y. Z., Ma, Y., & Wang, S. Y. (2007). Denitrification potential enhancement by addition of external carbon sources in a pre-denitrification process. *Journal of Environmental Sciences*, 19(3), 284–289. [https://doi.org/10.1016/S1001-0742\(07\)60046-1](https://doi.org/10.1016/S1001-0742(07)60046-1)

- Persson, T., Rudebeck, A., Jussy, J., Colin-Belgrand, M., Priemé, A., Dambrine, E., et al. (2000). Soil nitrogen turnover—Mineralisation, nitrification and denitrification in European forest soils. In E. Studies (Ed.), *Carbon and nitrogen cycling in European forest ecosystems* (pp. 297–311). Springer.
- Pianosi, F., Sarrazin, F., & Wagener, T. (2015). A matlab toolbox for global sensitivity analysis. *Environmental Modelling & Software*, 70, 80–85. <https://doi.org/10.1016/j.envsoft.2015.04.009>
- Piniewski, M., Marcinkowski, P., Koskiaho, J., & Tattari, S. (2019). The effect of sampling frequency and strategy on water quality modelling driven by high-frequency monitoring data in a boreal catchment. *Journal of Hydrology*, 579, 124186. <https://doi.org/10.1016/j.jhydrol.2019.124186>
- Prats, S., Malvar, M., Coelho, C., & Wagenbrenner, J. (2019). Hydrologic and erosion responses to compaction and added surface cover in post-fire logged areas: Isolating splash, interrill and rill erosion. *Journal of Hydrology*, 575, 408–419. <https://doi.org/10.1016/j.jhydrol.2019.05.038>
- Rhoades, C. C. (2019). Soil nitrogen leaching in logged beetle-killed forests and implications for riparian fuel reduction. *Journal of Environmental Quality*, 48(2), 305–313. <https://doi.org/10.2134/jeq2018.04.0169>
- Robichaud, P. R., Pierson, F. B., Brown, R. E., & Wagenbrenner, J. W. (2008). Measuring effectiveness of three postfire hillslope erosion barrier treatments, western Montana, USA. *Hydrological Processes: International Journal*, 22(2), 159–170. <https://doi.org/10.1002/hyp.6558>
- Rodman, K. C., Andrus, R. A., Butkiewicz, C. L., Chapman, T. B., Gill, N. S., Harvey, B. J., et al. (2021). Effects of bark beetle outbreaks on forest landscape pattern in the Southern Rocky Mountains, USA. *Remote Sensing*, 13(6), 1089. <https://doi.org/10.3390/rs13061089>
- Scheffer, M., Carpenter, S., Foley, J. A., Folke, C., & Walker, B. (2001). Catastrophic shifts in ecosystems. *Nature*, 413(6856), 591–596. <https://doi.org/10.1038/35098000>
- Schuldt, B., Buras, A., Arend, M., Vitasse, Y., Beierkuhnlein, C., Damm, A., et al. (2020). A first assessment of the impact of the extreme 2018 summer drought on Central European forests. *Basic and Applied Ecology*, 45, 86–103. <https://doi.org/10.1039/b823239c>
- Schwendenmann, L., & Michalzik, B. (2019). Dissolved and particulate carbon and nitrogen fluxes along a Phytophthora agathidicida infection gradient in a kauri (Agathis australis) dominated forest. *Fungal Ecology*, 42, 100861. <https://doi.org/10.1016/j.funeco.2019.08.005>
- Seidl, R., Schelhaas, M.-J., Rammer, W., & Verkerk, P. J. (2014). Increasing forest disturbances in Europe and their impact on carbon storage. *Nature Climate Change*, 4(9), 806–810. <https://doi.org/10.1038/nclimate2318>
- Shah, A. N., Tanveer, M., Shahzad, B., Yang, G., Fahad, S., Ali, S., et al. (2017). Soil compaction effects on soil health and crop productivity: An overview. *Environmental Science and Pollution Research*, 24(11), 10056–10067. <https://doi.org/10.1007/s11356-017-8421-y>
- Shaheeb, M. R., Venkatesh, R., & Shearer, S. A. (2021). A review on the effect of soil compaction and its management for sustainable crop production. *Journal of Biosystems Engineering*, 46(4), 417–439. <https://doi.org/10.1007/s42853-021-00117-7>
- Speich, M. J., Zappa, M., Scherstjanoi, M., & Lischke, H. (2020). FORests and HYdrology under climate change in Switzerland v1.0: A spatially distributed model combining hydrology and forest dynamics. *Geoscientific Model Development*, 13(2), 537–564. <https://doi.org/10.5194/gmd-13-537-2020>
- Sun, G., Wei, X., Hao, L., Sanchis, M. G., Hou, Y., Yousefpour, R., et al. (2023). Forest hydrology modeling tools for watershed management: A review. *Forest Ecology and Management*, 530, 120755. <https://doi.org/10.1016/j.foreco.2022.120755>
- Tan, X., Chang, S. X., & Kabzems, R. (2005). Effects of soil compaction and forest floor removal on soil microbial properties and N transformations in a boreal forest long-term soil productivity study. *Forest Ecology and Management*, 217(2–3), 158–170. <https://doi.org/10.1016/j.foreco.2005.05.061>
- Thomas, G., Rosalie, V., Olivier, C., & Antonio, L. P. (2021). Modelling forest fire and firebreak scenarios in a mediterranean mountainous catchment: Impacts on sediment loads. *Journal of Environmental Management*, 289, 112497. <https://doi.org/10.1016/j.jenvman.2021.112497>
- Tian, S., Youssef, M. A., Skaggs, R. W., Amatya, D. M., & Chescheir, G. M. (2012). Modeling water, carbon, and nitrogen dynamics for two drained pine plantations under intensive management practices. *Forest Ecology and Management*, 264, 20–36. <https://doi.org/10.1016/j.foreco.2011.09.041>
- UBA. (2022). Medienübergreifendes Monitoring in der Luftreinhaltung. Retrieved from <https://www.umweltbundesamt.de/themen/luft/messenbeobachteneuberwachen/medieneuegreifendes-monitoring-in-der#icp-integrated-monitoring>
- Ueda, M. U., Kachina, P., Marod, D., Nakashizuka, T., & Kurokawa, H. (2017). Soil properties and gross nitrogen dynamics in old growth and secondary forest in four types of tropical forest in Thailand. *Forest Ecology and Management*, 398, 130–139. <https://doi.org/10.1016/j.foreco.2017.05.010>
- Vacek, Z., Vacek, S., & Cukor, J. (2023). European forests under global climate change: Review of tree growth processes, crises and management strategies. *Journal of Environmental Management*, 332, 117353. <https://doi.org/10.1016/j.jenvman.2023.117353>
- Veldkamp, E., Schmidt, M., Powers, J. S., & Corre, M. D. (2020). Deforestation and reforestation impacts on soils in the tropics. *Nature Reviews Earth & Environment*, 1(11), 590–605. <https://doi.org/10.1038/s43017-020-0091-5>
- Vilhar, U., Kermavnar, J., Kozamernik, E., Petrič, M., & Ravbar, N. (2022). The effects of large-scale forest disturbances on hydrology—An overview with special emphasis on karst aquifer systems. *Earth-Science Reviews*, 235, 104243. <https://doi.org/10.1016/j.earscirev.2022.104243>
- Vrugt, J. A., ter Braak, C. J. F., Diks, C. G. H., Robinson, B. A., Hyman, J. M., & Higdon, D. (2009). Accelerating Markov chain Monte Carlo simulation by differential evolution with self-adaptive randomized subspace sampling. *International Journal of Nonlinear Sciences and Numerical Simulation*, 10(3), 273–290. <https://doi.org/10.1515/ijnsns.2009.10.3.273>
- Wei, X., & Zhang, M. (2010). Quantifying streamflow change caused by forest disturbance at a large spatial scale: A single watershed study. *Water Resources Research*, 46(12), W12525. <https://doi.org/10.1029/2010WR009250>
- Wellen, C., Kamran-Disfani, A.-R., & Arhonditsis, G. B. (2015). Evaluation of the current state of distributed watershed nutrient water quality modeling. *Environmental Science & Technology*, 49(6), 3278–3290. <https://doi.org/10.1021/es5049557>
- Wickenkamp, I., Huisman, J. A., Bogenia, H. R., Graf, A., Lin, H., Drüe, C., & Vereecken, H. (2016). Changes in measured spatiotemporal patterns of hydrological response after partial deforestation in a headwater catchment. *Journal of Hydrology*, 542, 648–661. <https://doi.org/10.1016/j.jhydrol.2016.09.037>
- Wirth, C., Schulze, E., Schwalbe, G., Tomczyk, S., Weber, G., Weller, E., et al. (2004). Dynamik der Kohlenstoffvorräte in den Wäldern Thüringens. *Abschlussbericht zur*, 1.
- Zema, D. A. (2021). Postfire management impacts on soil hydrology. *Current Opinion in Environmental Science & Health*, 21, 100252. <https://doi.org/10.1016/j.coesh.2021.100252>
- Zeppenfeld, T., Svoboda, M., DeRose, R. J., Heurich, M., Müller, J., Čížková, P., et al. (2015). Response of mountain picea abies forests to stand-replacing bark beetle outbreaks: Neighbourhood effects lead to self-replacement. *Journal of Applied Ecology*, 52(5), 1402–1411. <https://doi.org/10.1111/1365-2664.12504>
- Zhang, D., Hui, D., Luo, Y., & Zhou, G. (2008). Rates of litter decomposition in terrestrial ecosystems: Global patterns and controlling factors. *Journal of Plant Ecology*, 1(2), 85–93. <https://doi.org/10.1093/jpe/rtn002>

- Zhang, H., Wang, B., Li Liu, D., Zhang, M., Leslie, L. M., & Yu, Q. (2020). Using an improved SWAT model to simulate hydrological responses to land use change: A case study of a catchment in tropical Australia. *Journal of Hydrology*, 585, 124822. <https://doi.org/10.1016/j.jhydrol.2020.124822>
- Zheng, C., & Jia, L. (2020). Global canopy rainfall interception loss derived from satellite earth observations. *Ecohydrology*, 13(2), e2186. <https://doi.org/10.1002/eco.2186>
- Zimmermann, L., Moritz, K., Kennel, M., & Bittersohl, J. (2000). Influence of bark beetle infestation on water quantity and quality in the Grosse Ohe catchment (Bavarian Forest National Park). *Silva Gabreta*, 4(5), 1–62.